Human Molecular Genetics, 2009, Vol. 18, No. 20 ***3876–3893***
doi:10.1093/hmg/ddp331
Advance Access published on July 19, 2009

Neutralization of granulocyte macrophage colony-stimulating factor decreases amyloid beta 1-42 and suppresses microglial activity in a transgenic mouse model of Alzheimer's disease

Maria Manczak[1], Peizhong Mao[1], Kazuhiro Nakamura[2], Christopher Bebbington[3], Byung Park[4] and P. Hemachandra Reddy[1,5,*]

[1]Neurogenetics Laboratory and [2]Central Autonomic Regulation Laboratory, Division of Neuroscience, Oregon National Primate Research Center, 505 NW 185th Avenue, Beaverton, OR 97006, USA, [3]KaloBios Pharmaceuticals Inc., 260 E. Grand Avenue, South San Francisco, CA 94080, USA, [4]Division of Biostatistics, Department of Public Health and Preventive Medicine, Oregon Health and Science University, Portland, OR 97239, USA and [5]Department of Physiology and Pharmacology, Oregon Health and Science University, Portland, OR 97201, USA

Received April 29, 2009; Revised July 2, 2009; Accepted July 16, 2009

The purpose of our study was to investigate microglia and astrocytes that are associated with human mutant amyloid precursor protein and amyloid beta (Aβ). We investigated whether the anti-granulocyte–macrophage-colony stimulating factor (GM-CSF) antibody can suppress microglial activity and decrease Aβ production in Alzheimer's disease transgenic mice (Tg2576 line). An antibody to mouse GM-CSF was introduced by intracerebroventricular (ICV) injections into the brains of 10-month-old Tg2576 male mice. We assessed the effect of several GM-CSF-associated cytokines on microglial activities and their association with Aβ using quantitative real-time RT–PCR, immunoblotting, immunohistochemistry analyses in anti-GM-CSF antibody-injected Tg2576 mice. Using sandwich ELISA technique, we measured intraneuronal Aβ in Tg2576 mice injected with GM-CSF antibody and PBS vehicle-injected control Tg2576 mice. Using double-labeling immunofluorescence analysis of intraneuronal Aβ, Aβ deposits and pro-inflammatory cytokines, we assessed the relationship between Aβ deposits and microglial markers in the Tg2576 mice, and also in the anti-GM-CSF antibody-injected Tg2576 mice. Our real-time RT–PCR analysis showed an increase in the mRNA expression of IL6, CD11c, IL1β, CD40 and CD11b in the cerebral cortices of the Tg2576 mice compared with their littermate non-transgenic controls. Immunohistochemistry findings of microglial markers agreed with our real-time RT–PCR results. Interestingly, we found significantly decreased levels of activated microglia and Aβ deposits in anti-GM-CSF antibody-injected Tg2576 mice compared with PBS vehicle-injected Tg2576 mice. Findings from our real-time RT–PCR and immunoblotting analysis agreed with immunohistochemistry results. Our double-labeling analyses of intraneuronal Aβ and CD40 revealed that intraneuronal Aβ is associated with neuronal expression of CD40 in Tg2576 mice. Our quantitative sandwich ELISA analysis revealed decreased levels of soluble Aβ1-42 and increased levels of Aβ1-40 in Tg2576 mice injected with the anti-GM-CSF antibody, suggesting that anti-GM-CSF antibody alone decreases soluble Aβ1-42 production and suppresses microglial activity in Tg2576 mice. These findings indicating the ability of the anti-GM-CSF antibody to reduce Aβ1-42 and microglial activity in Tg2576 mice may have therapeutic implications for Alzheimer's disease.

*To whom correspondence should be addressed at: Neurogenetics Laboratory, Neuroscience Division, Oregon National Primate Research Center, West Campus, Oregon Health and Science University, 505 NW 185th Avenue, Beaverton, OR 97006, USA. Tel: +1 5034182625; Fax: +1 503 418 2501; Email: reddyh@ohsu.edu; reddyph@aol.com

INTRODUCTION

Alzheimer's disease (AD) is a late-onset, progressive neurodegenerative disorder characterized by the loss of memory and an impairment of multiple cognitive functions. The major pathological features in the brains of AD patients are the presence of extra-cellular amyloid beta (Aβ) plaques and intracellular neurofibrillary tangles (1–5). Recent biochemical, molecular and gene expression studies of AD postmortem brains and AD transgenic mouse models revealed that multiple pathways are involved in AD pathogenesis. These pathways include synaptic failure (6–8), mitochondrial oxidative damage (5,9–13) and inflammatory responses (3,14–20). Among these cellular changes, inflammatory responses are reported to be critically involved in AD pathogenesis (3).

Inflammation is caused by the proliferation of reactive astrocytes and microglia that have been observed in the brains of AD patients (14,21) and AD transgenic mice (15,16,22,23). Several recent studies found increased cytokines, including the GM-CSF, in the cerebrospinal fluid of AD patients (24,25). Furthermore, AD transgenic mice lines that overexpress amyloid precursor protein (APP) and Aβ exhibit significant cerebrovascular inflammation and microgliosis around areas of Aβ plaque deposition (26–28). In addition, the chronic administration of ibuprofen and other non-steroidal anti-inflammatory drugs have been reported to reduce Aβ plaque pathology and Aβ levels in the brains of AD mice (29,30).

Microglia cells are associated with most Aβ plaques (31–33). Microglial activation involves proliferation of microglia cells, their homing to the site of injury and functional changes, including the release of cytotoxic and inflammatory mediators. Activated microglia may participate in the brain tissue damage in patients with AD. In an early stage of AD, microglia cells may perform synaptic stripping, leading to extensive synaptic damage in AD brains. Activation of glial cells is accompanied by an upregulation of APP expression, leading to Aβ accumulation in the chronic stage of the disease (14). Microglia can also act as a cytotoxic effector in cells by releasing proteases, reactive oxygen intermediates and nitric oxide (34) and by mediating neuronal injury (35). In addition, microglia can participate in an inflammatory response by acting as antigen-presenting cells to activate T-lymphocytes (36) and by producing pro-inflammatory cytokines, such as GM-CSF.

Among several cytokines found in the brains and cerebrospinal fluid of AD patients, GM-CSF is a pro-inflammatory cytokine, involved in the regulation of proliferation, differentiation and functional activities of granulocyte–macrophage populations (37). GM-CSF infusion in the brain depicts a dramatic proliferation of a large number of microglial cells (38,39). Indeed, GM-CSF is one of the strongest microglial mitogens (34,40,41). In addition, withdrawal of GM-CSF significantly enhances the death rate of microglial cells, as determined by a DNA fragmentation assay. Thus, increased levels of GM-CSF found in the cerebral spinal fluid of AD patients may play a crucial role in inducing microgliosis that typically occurs in the brains of patients with severe AD (24).

Recently, several studies focused on decreasing the Aβ load in AD transgenic mice by using active and passive immunizations (42–45). Several other studies treated AD transgenic mice using a combination of antibodies of Aβ and cytokines (GM-CSF and IL4) (39,46,47). Kim *et al*. (46) focused on intranasal immunization of adenovirus vectors encoding GM-CSF and Aβ in Tg2576 mice (an AD mouse model) and found decreased Aβ loads in the brains of the vaccinated Tg2576 mice compared with those in the control Tg2576 mice. DaSilva *et al*. (39) investigated the same combinational immunization approach (Aβ/GM-CSF/IL4) in APP mice that Kim *et al*. (46) used and found Aβ/GM-CSF/IL4 antibodies decreased ∼43% in the Aβ plaque load of AD transgenic mice, suggesting that the combinational approach may be effective in Aβ immunotherapy. Frazer *et al*. (47) used an amplicon (HSV-IE-Aβ(CMV)IL4) to co-deliver Aβ1-42 and interleukin-4 in a triple AD transgenic mice and found increased Aβ-specific antibodies, improved learning and improved functioning of memory and decreased AD pathology in the HSV(IE)Aβ(CMV)IL4-vaccinated mice compared with the other experimental groups. However, it is unclear whether anti-GM-CSF antibodies alone can suppress glial activity and can decrease Aβ pathology in AD transgenic mice.

We propose that anti-GM-CSF antibody suppresses microglial activity and decreases microglial-associated Aβ production and deposits in the brains of AD mice. To test these hypotheses, we investigated the microglial activity, Aβ production and Aβ deposits in a well-characterized APP transgenic mice (Tg2576 mice) after treating them with the anti-GM-CSF anti-mouse antibody. We injected this antibody into the brains of 10-month-old Tg2576 mice and a PBS vehicle into the brains of 10-month-old Tg2576 mice as a negative control, using ICV injections. We measured (i) mRNA expression of markers of microglia, astrocytes and neurons using SYBR-Green chemistry-based quantitative real-time RT–PCR, (ii) immunoblotting analysis of microglial markers, (iii) soluble and insoluble Aβ levels using sandwich ELISA, (iv) immunohistochemistry and immunofluorescence analyses of several markers of microglia, astrocytes and neurons, (v) Aβ deposits in the brains of Tg2576 mice injected with anti-GM-CSF antibody and/or the PBS vehicle, and (vi) examined the connection between intraneuronal Aβ/Aβ deposits and microglial activation.

RESULTS

mRNA expression of markers of microglia, astrocytes in 10-month-old male Tg2576 mice and non-transgenic mice

The objective of our study was to investigate the markers of microglia and astrocytes and their association with Aβ production and Aβ deposits in AD transgenic mice. We investigated the extent of mRNA in the cerebral cortex for markers of microglia, astrocytes and neurons (using quantitative real-time RT–PCR) and soluble and insoluble Aβ production (using sandwich ELISA) and Aβ deposits using immunohistochemistry and immunofluorescence analyses in 10-month-old male Tg2576 mice and age-matched, non-transgenic littermates.

As shown in Table 1, we found a 4.70-fold increase in mRNA levels for IL6, followed by a 4.02-fold increase for CD11c, a 2.24-fold increase for IL1β, a 1.39-fold increase for CD40 and a 1.2-fold increase for CD11b in the cerebral cortex tissues of 10-month-old male Tg2576 mice compared

Table 1. mRNA expression of microglial and neuronal markers between Tg2576 mice and age-matched littermates, and between PBS vehicle-injected Tg256 mice and anti-GM-CSF antibody-injected Tg2576 mice (β-actin normalization)

Marker	mRNA fold-change difference between 10-month-old Tg2576 mice and 10-month-old non-transgenic littermates	mRNA fold-change difference between 10-month-old PBS-injected Tg2576 mice and anti-GM-CSF antibody-injected 10-month-old Tg2576 mice
TNFα	0.68	0.44
IL1β	2.24	0.26
IL6	4.70	0.05
Gp91	0.40	1.47
CD11b	1.20	0.11
CD11c	4.02	1.48
CD40	1.39	0.31
CD45	0.90	0.56
MHCII -2	0.45	2.12
GFAP	1.30	1.64
NeuN	1.14	1.43

One-fold mRNA expression means no change between Tg2576 mice and non-transgenic littermates, and between PBS vehicle-injected Tg2576 mice and anti-GM-CSF antibody-injected Tg2576 mice; >1-fold mRNA expression indicates increased abundance to control mice and <1-fold mRNA expression, decreased abundance to control mice.

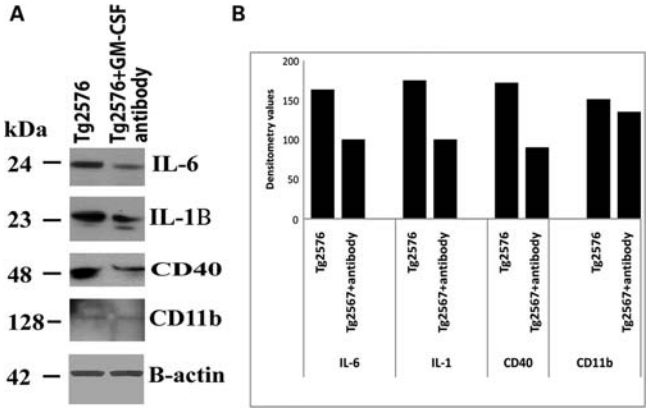

Figure 1. Immunoblotting analysis of microglial proteins in Tg2576 mice injected with GM-CSF antibody and Tg2576 mice injected with PBS. (**A**) Twenty micrograms of protein lysate was used from each sample, and immunoblotting analysis was performed using antibodies of IL1β, IL6, CD40 and β-actin. Bottom panel represents the immunoblotting of β-actin for equal loading. (**B**) Densitometry values for microglial proteins IL1β, IL6 and CD40 in Tg2576 mice injected with GM-CSF antibody and Tg2576 mice injected with PBS. As shown, we found decreased protein levels for CD40 (by 48%), followed by IL1β (43%), IL6 (39%) and CD11b (11%) in Tg2576 mice injected with GM-CSF antibody compared with Tg2576 mice injected with PBS.

with the non-transgenic control mice, suggesting that inflammatory responses are evident in overexpressed human mutant APP transgenic mice. We found a 1.30-fold increased mRNA expression for GFAP and a 1.14-fold increase for NeuN in the cerebral cortex tissues of 10-month-old Tg2576 mice compared with the non-transgenic control mice. We also found mRNA levels unchanged or slightly decreased for several other cytokine markers, such as CD45, TNFα, gp91 and MHCII in Tg2576 mice compared with the non-transgenic littermates.

mRNA expression of markers of microglia, astrocytes and neurons in PBS-injected Tg2576 mice and anti-GM-CSF antibody-injected Tg2576 mice

We sought to determine whether anti-GM-CSF antibody can suppress the activated microglial activity that was observed in overexpressed mutant human APP transgenic mice. Therefore, we investigated mRNA levels of pro-inflammatory cytokines in anti-GM-CSF antibody-injected Tg2576 mice compared with PBS-injected Tg2576 mice.

As shown in Table 1, interestingly, we found decreased mRNA levels of IL1β, IL6, CD11b, CD11c and CD40 in anti-GM-CSF antibody-injected Tg2576 mice compared with the PBS vehicle-injected Tg2576 mice. mRNA levels were increased for IL1β, IL6, CD11b, CD11c and CD40 in the Tg2576 mice compared with the non-transgenic wild-type mice, and these increased mRNA levels were decreased in anti-GM-CSF antibody-injected Tg2576 mice, suggesting that anti-GM-CSF antibody suppressed the activated microglia in the Tg2576 mice. We also noticed that slightly increased mRNA levels for GFAP (1.64-fold) and MHCII-2 (2.12-fold) in the anti-GM-CSF antibody-injected Tg2576 mice compared with the PBS vehicle-injected Tg2576 mice.

Immunoblotting analysis of proteins of microglial markers in Tg2576 mice injected with GM-CSF antibody and Tg2576 mice injected with PBS vehicle

To determine whether GM-CSF antibody reduces protein levels of microglial markers that are associated with Aβ deposits in AD, we performed immunoblotting analysis of markers of microglia, IL1β, IL6, CD40 and CD11b in protein lysates prepared from cerebral cortices of Tg2576 mice injected with GM-CSF antibody and Tg2576 mice injected with PBS vehicle. As shown in Figure 1, we found decreased protein levels for CD40 (by 48%), followed by IL1β (43%), IL6 (39%) and CD11b (11%) in Tg2576 mice injected with GM-CSF antibody compared with Tg2576 mice injected with PBS vehicle (control), suggesting that GM-CSF antibody reduced proteins of microglia associated with Aβ deposits in Tg2576 mice. These findings agreed with the results of real-time RT–PCR and immunohistochemistry analysis.

Immunohistochemistry and immunofluorescence analyses of markers of microglia and GFAP in Tg2576 mice and non-transgenic wild-type mice

To determine whether overexpressed mutant APP and Aβ deposits activate microglia and astrocytes, we conducted immunohistochemistry and immunofluorescence analyses of several glial markers, including IL1β, IL6, CD11b, CD11c, TNFα and CD40, in the Tg256 mice and in the non-transgenic, wild-type mice. We found increased immunoreactivity of IL1β (Fig. 2), IL6 (Supplementary Material, Fig. S1), CD11c (Supplementary Material, Fig. S2) and CD11b (Supplementary Material, Fig. S3) in the hippocampal and cortical regions, where Aβ deposits abundantly found in 10-month-old Tg2576 mice compared with the age-matched, non-transgenic mice (data not shown because of low or undetectable immunoreactivity).

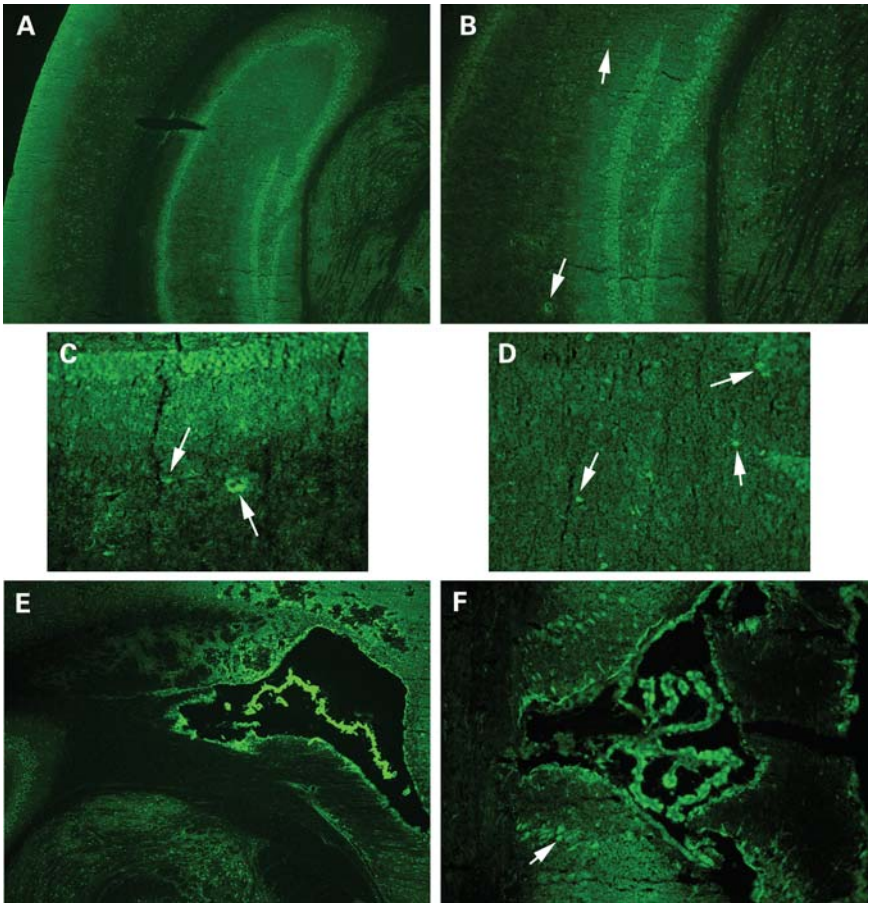

Figure 2. Immunoreactivity of IL1 in different brain regions of a representative Tg2576 mouse. Accumulated immunoreactivity was found in the cerebral cortex, hippocampus and ventricular regions of the brain in Tg2576 mice. Arrows indicate the increased immunoreactivity of IL1β in the hippocampus, layers 1–3 in the cortex and ventricular regions of the midbrain. (**A**) Photographed at ×5 the original magnification, (**B**) ×10, (**C** and **D**) ×20, (**E** and **F**) ×10.

Double-labeling analyses of intraneuronal Aβ, Aβ deposits and microglia, astrocytes and CD40

Our double-labeling immunohistochemistry and immunofluorescence analyses of Aβ deposits and activated microglia in Tg2576 mice revealed: (i) Aβ deposits are surrounded by microglia, marked by immunoreactivity of IL1β (Fig. 3A) and CD11b (Fig. 3B), (ii) Aβ deposits are present without microglia marked by immunoreactivity of IL6 (Fig. 4A) and CD11b (Fig. 4B), (iii) Aβ deposits are surrounded by astrocytes (Fig. 5), suggesting that microglial and astrocytic activation are dependent on the presence of Aβ deposits, and also Aβ deposits are present without microglial association.

Our double-labeling analysis of intraneuronal Aβ and CD40 revealed that intraneuronal Aβ is co-localized with the immunoreactivity of CD40 in neurons (Fig. 6), suggesting that co-localization of intraneuronal Aβ and CD40 triggers abnormal APP processing and increased pro-inflammatory cytokine production in Tg2576 mice.

Double-labeling analyses of CD40 and NeuN

To determine whether CD40 is expressed in neurons, we performed double-labeling analyses of NeuN and CD40 in the brain sections from Tg2576 mice. Our double-labeling immunohistochemistry and immmunofluorescence analyses revealed that CD40 is expressed in some neurons and co-localized with NeuN (Fig. 7). However, we also found several NeuN-positive neurons did not show CD40 expression, indicating that some neurons selectively expressed for CD40 in the brains of Tg2576 mice. This finding further supports the presence of intraneuronal expression of CD40 and Aβ in Tg2576 mice (Fig. 6).

Aβ production in anti-GM-CSF antibody-injected Tg2576 mice and PBS-injected Tg2576 mice

To determine whether anti-GM-CSF antibody can reduce Aβ production, using sandwich ELISA we measured both soluble and insoluble Aβ1-40 and Aβ1-42 levels in anti-GM-CSF antibody-injected Tg2576 mice and PBS-injected Tg2576 mice. Interestingly, for the first time, we found decreased levels of soluble Aβ1-42 (46%) in Tg2576 mice injected with anti-GM-CSF antibody compared with Tg2576 mice injected with PBS (control). However, these decreased levels of Aβ1-42 in GM-CSF-injected Tg2576 mice are not statistically significant ($P < 0.28$) (Table 2), and this insignificant difference may be due to a small number of animals studied in each group.

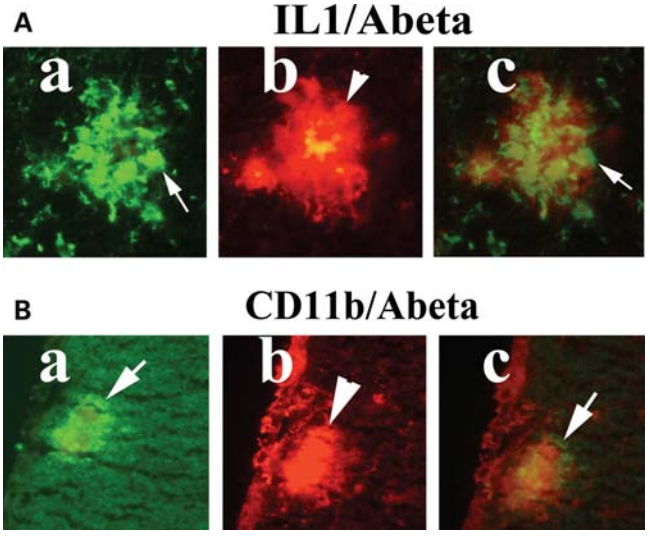

Figure 3. Double-labeling immunofluorescence analyses of Aβ deposit and microglia marked by IL1β (**A**) and CD11b (**B**) in representative 10-month-old Tg2576 mouse. Aβ deposits are associated with microglia. (Aa) Immunoreactivity of IL1, (Ab) surrounded by Aβ deposit in the same section and (Ac) overlay of both IL1 and Aβ deposit. Arrows indicate immunoreactivity of IL1 (in white), and the arrowhead indicates Aβ deposit. (Ba) Immunoreactivity of CD11b, (Bb) surrounded by Aβ deposit and (Bc) overlay of both CD11b and Aβ deposit. Arrows indicate immunoreactivity of CD11b (in white), and the arrowhead indicate Aβ deposit.

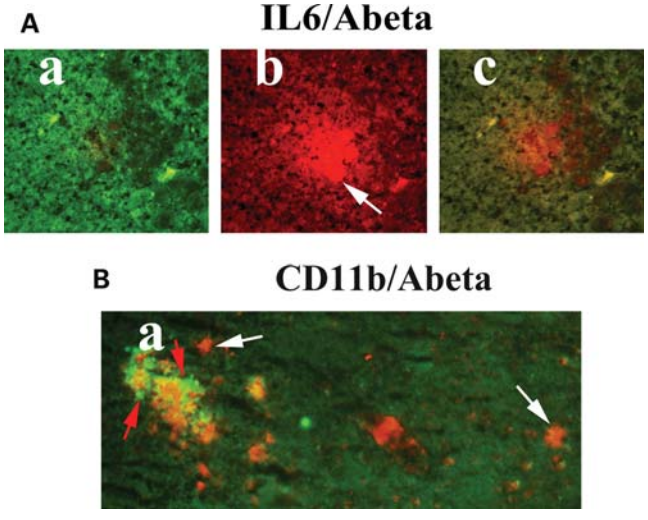

Figure 4. Double-labeling immunofluorescence analyses of Aβ deposit and microglia marked by IL6 (**A**) and CD11b (**B**) in a representative10-month-old Tg2576 mouse. Aβ deposit without microglia. (A) Microglia marked by immunoreactivity of IL6 (a), Aβ deposit without microglia in the same section (b) and overlay of both IL6 and Aβ deposit (c). (B) Immunoreactivity of microglia marked by CD11b present in the vicinity of Aβ deposit (arrows in white). Aβ deposits are present without microglial immunoreactivity of CD11b (arrows in red).

In addition, we also found increased levels of soluble Aβ1-40 (23%) and insoluble Aβ1-40 (27%) in anti-GM-CSF antibody-injected Tg2576 mice compared with the PBS-injected Tg2576 mice. However, these increased levels of soluble Aβ1-40 ($P < 0.44$) and insoluble Aβ1-40 ($P < 0.18$) are not statistically significant (Table 2).

However, overall, these findings indicate that the anti-GM-CSF antibody interferes with soluble Aβ1-42 production and/or clear soluble Aβ1-42 more rapidly in AD transgenic mice, which in turn may have implications for the use of the anti-GM-CSF antibody as a therapy for AD patients.

Immunohistochemistry and immunofluorescence analyses of markers of microglia in anti-GM-CSF antibody-injected Tg256 mice and PBS-injected Tg2576 mice

To determine whether anti-GM-CSF antibody can suppress microglial activity (caused by overexpressed mutant APP and Aβ deposits), we conducted immunohistochemistry and immunofluorescence analyses of several glial markers, including IL1β, IL6, CD11b, CD11c, TNFα and CD40 in PBS vehicle-injected Tg256 mice and anti-GM-CSF antibody-injected Tg2576 mice.

We found a statistically significant decreased immunoreactive signal intensity for IL6 ($P < 0.0016$) (Fig. 8), CD11c ($P < 0.0001$) (Fig. 9) and CD40 ($P < 0.0001$) in anti-GM-CSF antibody-injected Tg2576 mice compared with PBS vehicle-injected Tg2576 mice, suggesting that GM-CSF antibody suppress microglial activity in Tg2576 mice. We also found decreased but not significant immunoreactivity for IL1β, CD11b, TNFα in anti-GM-CSF antibody-injected Tg2576 mice compared with the PBS vehicle-injected Tg2576 mice .

We found slightly increased immunoreactivity of GFAP (Fig. 10) in anti-GM-CSF antibody-injected Tg2576 mice compared with the PBS vehicle-injected Tg2576 mice. Interestingly, we found slightly increased but not significant immunoreactivity of GFAP in GM-CSF antibody-injected Tg2576 mice compared with PBS vehicle-injected Tg2576 mice (Fig. 10), suggesting GM-CSF antibody has little or no effect on GFAP.

Immunohistochemistry and immunofluorescence analyses of intraneuronal Aβ and Aβ deposits in anti-GM-CSF antibody-injected Tg256 mice and PBS-injected Tg2576 mice

To determine whether the anti-GM-CSF antibody reduces Aβ deposits, we conducted immunohistochemistry and immunofluorescence analyses of Aβ deposits in PBS-injected Tg256 mice and anti-GM-CSF antibody-injected Tg2576 mice.

We found a statistically significant decreased Aβ deposits ($P < 0.01$) (Fig. 11) in anti-GM-CSF antibody-injected Tg2576 mice compared with PBS vehicle-injected Tg2576 mice, suggesting that GM-CSF antibody decreases microglial-associated Aβ deposits in Tg2576 mice.

DISCUSSION

The purpose of our study was to investigate pro-inflammatory cytokines that are associated with human APP Swedish mutation(s) in AD, and to investigate whether the anti-GM-CSF antibody can suppress microglial activity induced by human APP mutation in Tg2576 mice. Using ICV injections, we injected the anti-GM-CSF antibody or the PBS vehicle into the brains of Tg2576 mice. Using quantitative real-time RT–PCR,

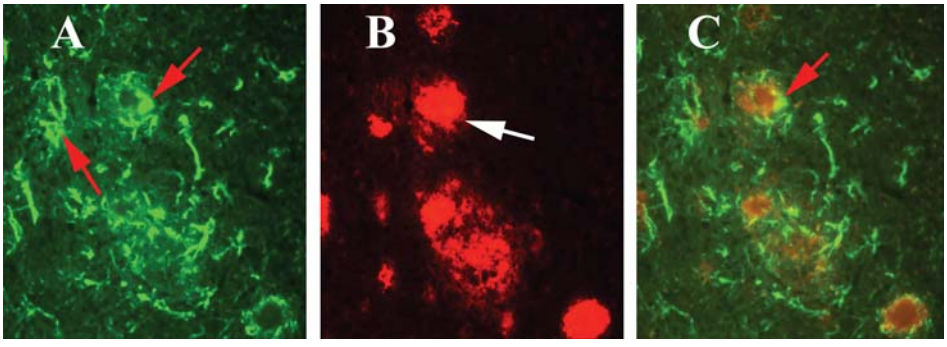

Figure 5. Double-labeling immunofluorescence analyses of Aβ deposit and astrocytes marked by glial fibrillary acidic protein (GFAP) in a representative 10-month-old Tg2576 mouse. (**A**) Immunoreactivity of GFAP (in green), (**B**) immunoreactivity of Aβ deposits (in red) of the same section and (**C**) overlay of GFAP and Aβ deposits. Aβ deposits are associated with astrocytes.

we measured mRNA levels of several GM-CSF-associated cytokines in Tg2576 mice, non-transgenic wild-type mice, PBS vehicle-injected mice and anti-GM-CSF antibody-injected Tg2576 mice. We measured soluble and insoluble Aβ1-40 and Aβ1-42 in PBS vehicle-injected and anti-GM-CSF antibody-injected Tg2576 mice. Using immunoblotting analysis, we studied the protein levels of microglial markers in PBS vehicle-injected and anti-GM-CSF antibody-injected Tg2576 mice. Using immunohistochemistry and immunofluorescence, we assessed intraneuronal Aβ and Aβ deposits. Using double-labeling immunofluorescence analysis, we assessed the relationship between Aβ deposits and markers of microglia and astrocytes in anti-GM-CSF antibody-injected Tg2576 mice and PBS vehicle-injected Tg2576 mice. Our real-time RT–PCR analysis showed an increased mRNA expression of IL6, CD11c, IL1, CD40 and CD11b in the cerebral cortices of the Tg2576 mice compared with the non-transgenic wild-type mice. Further, the anti-GM-CSF antibody significantly suppressed the human APPswe mutation and deposits of Aβ-induced glial activity in the brains of Tg2576 mice. Our immunoblotting and immunohistochemistry findings of microglial markers in Tg2576 mice injected with GM-CSF antibody concur with our real-time RT–PCR findings. In Tg2576 mice, we found Aβ deposits are surrounded by microglia and astrocytes, and intraneuronal Aβ co-localized with intraneuronal CD40. These results suggest that intraneuronal expression of Aβ may activate the expression of CD40 in AD neurons. Interestingly for the first time, we found decreased levels of soluble Aβ1-42 and increased levels of Aβ1-40 in Tg2576 mice injected with anti-GM-CSF antibody, indicating that anti-GM-CSF antibody clears the levels of soluble Aβ1-42 more rapidly and/or decreases the production of soluble Aβ1-40.

IL6 and AD

IL6 is a pro-inflammatory cytokine that is secreted by T cells and macrophages to stimulate immune response to trauma or tissue damage leading to inflammation. IL6 is activated in AD brains (48–50). In the present study, IL6 mRNA in Tg2576 mice was the most upregulated among all pro-inflammatory cytokines that we examined in this study. This result is supported by several previous studies of AD postmortem brains (48–50) and AD transgenic mice (15,16,51–56). Ravaglia *et al*. (48) found increased serum IL6 associated with vascular dementia. Together, findings from our study and the studies of AD postmortem brains, AD transgenic mice and serum from AD patients suggest that increased IL6 is involved in AD progression.

Our immunohistochemistry analysis of IL6 in Tg2576 mice injected with the anti-GM-CSF antibody and PBS vehicle-injected Tg2576 mice revealed that overexpressed IL6 is significantly suppressed by anti-GM-CSF antibody in the brain regions, including cortex and hippocampus of Tg2576 mice ($P < 0.0016$), suggesting that anti-GM-CSF antibody is a potent suppresser of IL6 in Tg2576 mice. Our real-time RT–PCR (Table 1) and immunoblotting findings (Fig. 1) also showed decreased mRNA and protein levels of IL6 in Tg2576 mice injected with GM-CSF antibody, which further supports that GM-CSF antibody is a suppressor of IL6 in AD transgenic mice.

CD11b and AD

CD11b is also known as heterodimeric integrin alpha-M beta-2 and is expressed on the surface of many leukocytes involved in the innate immune system, including monocytes, granulocytes, macrophages. CD11b mediates inflammation by regulating leukocyte adhesion and migration. CD11b is reported to be activated in AD brains, and in the present study, we found increased mRNA expression in the cerebral cortex of Tg2576 mice compared with control mice. We also found increased immunoreactivity in the brains of Tg2576 mice, mainly in the vicinity of Aβ deposits (Supplementary Material, Fig. S3), suggesting that CD11b is activated in response to increased Aβ deposits. Our findings are supported by several previous studies in AD brains (57,58) and AD transgenic mice (54,59–61).

Our immunohistochemistry analysis of CD11b in Tg2576 mice injected with anti-GM-CSF antibody showed decreased but not significant CD11b immunoreactivity in the hippocampal and cortical regions, particularly in the vicinity of Aβ deposits, indicating that GM-CSF antibody suppresses the microglial activity as shown by CD11b expression in Tg2576 mice. Findings from our real-time RT–PCR (Table 1) and immunoblotting (Fig. 1) also showed decreased mRNA and protein levels of CD11b in Tg2576 mice injected

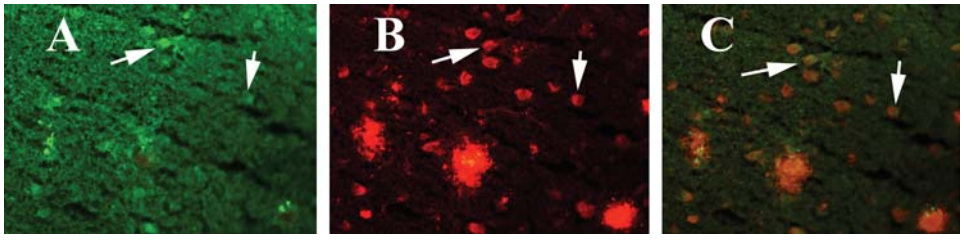

Figure 6. Double-labeling analysis of intraneuronal Aβ and CD40 in a representative 10-month-old Tg2576 mouse. (**A**) Immunoreactivity of CD40 (in green), (**B**) intraneuronal Aβ and Aβ deposits (in red) of the same section and (**C**) overlay of CD40 and intraneuronal Aβ. Arrows indicate localization of intraneuronal Aβ and CD40. Sections were photographed at ×40 the original magnification.

with GM-CSF antibody, which further supports that GM-CSF antibody is a suppressor of CD11b in AD transgenic mice.

CD11c and AD

CD11c is a type-I transmembrane protein found in dendritic cells, monocytes, macrophages, neutrophils and beta cells. Our finding of increased mRNA expression of CD11c in Tg2576 mice relative to control mice has been reported in AD postmortem brains (62,63) and AD transgenic mouse lines (60,64) and cell culture studies of microglia activated by aggregated Aβ (65). de Groot *et al*. (66) developed cultures of microglial cells from rapid autopsies of the subcortical white matter, corpus callosum and frontal, temporal and occipital cortex (range 3–10 h) of non-demented elderly individuals and AD patients and found that the adherent microglial cells were immunoreactive for CD68, CD45, CD11c and MHCII markers. Upon the stimulation with lipopolysaccharide, microglial cells secreted pro- and anti-inflammatory mediators, IL6, prostaglandin E2 and IL10, suggesting the functional capacity of cultured microglia from AD patients (66). These findings further support our observations that CD11c is abnormally expressed in the Tg2576 mice. We found that upregulated CD11c is significantly suppressed by the anti-GM-CSF antibody in Tg2576 mice ($P < 0.0001$). Further, our real-time RT–PCR findings (Table 1) also showed decreased mRNA levels of CD11c in Tg2576 mice injected with GM-CSF antibody, which further supports that GM-CSF antibody is a suppressor of CD11c in AD transgenic mice.

IL1β and AD

IL1β is produced by macrophages, monocytes and dendritic cells, and IL1β forms an important part of the inflammatory response of the body against infection, particularly in disease state such as Alzheimer's. IL1β increases the expression of adhesion factors on endothelial cells to the cells that fight pathogens. In the present study, we found increased mRNA expression of IL1β in Tg2576 mice, and our findings are supported by data from AD patients (67). Increased levels of IL1β were found to be associated with plaques in AD (68). Further, Guillemin *et al*. (68) found that Aβ induces IL1β mRNA expression in human fetal astrocytes and macrophages. Combs *et al*. (69) reported a functional relationship between Aβ-dependent activation of microglia and several characteristic markers of neuronal death occurring in AD brains. Findings from AD postmortem studies, together with our present study, suggest that IL1β upregulation may be a characteristic of AD.

Our immunohistochemistry analysis of IL1β in Tg2576 mice injected with GM-CSF antibody showed suppressed overexpression of IL1β in Tg2576 mice, further suggesting that the anti-GM-CSF antibody may have anti-inflammatory therapeutic value in AD. Our real-time RT–PCR (Table 1) and immunoblotting findings (Fig. 1) also showed decreased mRNA and protein levels of IL1β in Tg2576 mice injected with GM-CSF antibody, which further supports that GM-CSF antibody is a suppressor of IL1β in AD transgenic mice.

CD40 and AD

The increased CD40 expression that we found in Tg2576 mice compared with the control mice is supported by several studies (70–72).

CD40 is a cell-surface marker and a member of the tumor necrosis factor receptor super-family, reported to play a role in the metabolism of Aβ in AD pathogenesis (70–72). Buchhave *et al*. (70) investigated the plasma levels of soluble CD40 and the soluble CD40 ligand in 136 subjects with mild cognitive impairment (MCI) and in 30 age-matched controls. Sixty of the 136 MCI cases progressed to AD during a clinical follow-up period of 4–7 years. The baseline levels of soluble CD40 were elevated in the MCI-AD cases compared with age-matched controls, suggesting that CD40 may play a role in the pathogenesis of early AD.

Ait-ghezala *et al*. (72) measured plasma Aβ, soluble CD40 and soluble CD40 ligand levels in 73 AD patients and compared their levels with those of 102 controls. They found increased levels of Aβ1-40, insoluble CD40 and the soluble CD40 ligand in the AD patients, suggesting that CD40 and the CD40 ligand are associated with AD progression. Recently, Volmer *et al*. (71) have shown increased levels of Aβ in human embryonic kidney cells overexpressing both mutant APP and CD40. Further, they demonstrated that GM-CSF-neutralizing antibodies mitigate the CD40L-induced production of Aβ in human embryonic kidney cells expressing human mutant APP and CD40. They also showed that shRNA silencing of the GM-CSF receptor gene significantly reduced Aβ levels below the baseline in non-stimulated HEK/APPsw/CD40 cells. Analysis of cell-surface proteins revealed that silencing of the GM-CSF receptor also decreased APP endocytosis. Overall, findings from the Volmar *et al*. (71) study agree with our present study and suggest a role for GM-CSF in Tg2576 mice.

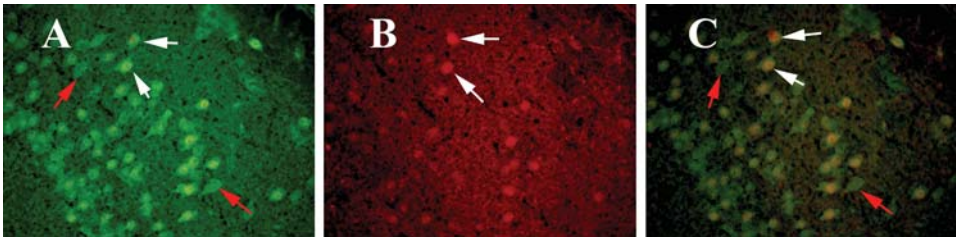

Figure 7. Double-labeling analysis of intraneuronal NeuN and CD40 in a representative 10-month-old Tg2576 mouse. (**A**) Immunoreactivity of NeuN (in green) in the cerebral cortex section, (**B**) intraneuronal CD40 (in red) of the same section and (**C**) overlay of NeuN and CD40. White arrows indicate co-localized neurons with NeuN and CD40, and red arrows indicate neurons only with NeuN expression. Sections were photographed at $\times 40$ the original magnification.

Obregon *et al*. (73) used genetic and pharmacological approaches to determine whether a CD40–CD40L blockade could enhance the efficacy of an Aβ1-42 immunization. They found that the genetic or pharmacological interruption of the CD40–CD40L interaction enhanced Aβ1-42 immunization efficacy and reduced cerebral amyloidosis in the PSAPP and Tg2576 mouse models of AD (73).

Laporte *et al*. (74) have generated APP and PSAPP mouse models with a disrupted CD40 gene. They compared the pathological features of AD with appropriate controls and found all these features reduced in mouse models deficient in CD40 compared with their controls that were not deficient in CD40, suggesting that CD40 signaling is required to allow the full repertoire of AD-like pathology in Tg2576 mice, and that the inhibition of the CD40 signaling pathway may be a potential therapeutic strategy in AD. In another study, Nichol *et al*. (75) investigated whether exercise could alter the immune profile in 17–19-month-old Tg2576 mice to a response that reduces Aβ pathology. They found decreased levels of ILβ and TNFα and increased levels of CD40 and MHCII in exercised animals compared with sedentary mice. These results suggest that CD40 and other cytokines are associated with AD pathogenesis.

Our immunohistochemistry analysis of CD40 in Tg2576 mice injected with anti-GM-CSF antibody showed significantly decreased CD40 immunoreactivity ($P < 0.0001$) in the hippocampal and cortical regions, indicating that GM-CSF antibody suppresses the microglial activity as shown by CD40 expression in Tg2576 mice. Findings from our real-time RT–PCR (Table 1) and immunoblotting (Fig. 1) also showed decreased mRNA and protein levels of CD40 in Tg2576 mice injected with GM-CSF antibody, which further supports that GM-CSF antibody is a suppressor of CD40 in AD transgenic mice. Overall, findings from AD postmortem brains, AD mice and cell-line studies on CD40 and GM-CSF support our present study observations, which suggests that GM-CSF and CD40 play a large role in AD pathogenesis.

Association of intraneuronal Aβ and CD40

We found co-localization of CD40 and intraneuronal Aβ in Tg2576 mice. We further confirmed intraneuronal expression of CD40 using double-labeling analyses of NeuN and CD40 in brain sections from Tg2576 mice. However, there are no published reports in AD mice and AD patients on the co-localization of CD40 and intraneuronal Aβ. In a recent paper, Hou *et al*. (76) reported that CD40 is expressed in neurons. The intraneuronal expression of CD40 and its connection with intraneuronal Aβ in AD are still unclear. However, it is possible that the interaction between intraneuronal Aβ and CD40 may promote inflammation via cytokine activation, in addition to increasing Aβ deposits associated with cytokines. It is also possible that interaction between intraneuronal Aβ and CD40 may promote abnormal APP processing and generate increased production of Aβ1-42. We also found decreased co-localization of intraneuronal Aβ in Tg2576 mice injected with the anti-GM-CSF antibody, suggesting that GM-CSF antibody may decrease intraneuronal expression of CD40 in Tg2576 mice.

GFAP and GM-CSF in Tg2576 mice

We found increased mRNA abundance of GFAP and increased astrocytes in our immunohistochemistry in Tg2576 mice compared with non-transgenic littermates, and our observations are supported by Lim *et al*. (29). However, there is a slight increase of GFAP expression in Tg2576 mice injected with GM-CSF antibody in Tg2576 mice relative to PBS vehicle-injected Tg2576 mice. The precise link between increased levels of GFAP and anti-GM-CSF antibody in Tg2576 mice is unclear. Further research is needed to investigate the connection between increased GFAP and anti-GM-CSF antibody in APP mice.

However, as described earlier, we found suppressed microglial activity and decreased intraneuronal Aβ1-42 levels and Aβ deposits in anti-GM-CSF antibody-injected Tg2576 mice relative to PBS vehicle-injected Tg2576 mice, suggesting that anti-GM-CSF antibody may have a potential therapeutic value for AD.

GM-CSF treatment and decreased Aβ1-42

There are no published reports thus far to compare our present findings of decreased Aβ1-42 levels and increased Aβ1-40 in AD transgenic mice with the administration of the anti-GM-CSF antibody directly into the mouse brain. However, there have been studies conducted using an adenovirus vaccine of both GM-CSF and Aβ (46,77). Zou *et al*. (77) injected vaccine-expressing $4 \times$Aβ (1–15) and gene-adjuvant GM-CSF into Tg2576 mice. The adenovirus vaccine induced an Aβ-specific IgG1-predominant humoral immune response and reduced Aβ deposits in Tg2576 mice and reduced cognition deficits.

Using a vaccine with an adenovirus vector encoding GM-CSF and Aβ, Kim *et al*. (46) studied Aβ deposits in Tg2576 mice.

Table 2. Summary of beta amyloid levels between PBS vehicle-injected Tg256 mice and anti-GM-CSF antibody-injected Tg2576 mice using sandwich ELISA

Number of mice	Soluble Aβ1-40 (pg/mg), mean ± SE	*P*-value	%Difference	Soluble Aβ1-42 (pg/mg), mean ± SE	*P*-value	%Difference	Insoluble Aβ1-40 (pg/mg), mean ± SE	*P*-value	%Difference	Insoluble Aβ1-42 (pg/mg), mean ± SE	*P*-value	%Difference
Tg2576 ($n = 5$)	6.4 ± 1.79	0.44	23% increased in anti-GM-CSF-injected mice	5.4 ± 1.1	0.28	46% decreased in anti-GM-CSF-injected mice	0.6 ± 0.11	0.18	27% increased in anti-GM-CSF-injected mice	0.28 ± 0.09	0.9	No change
Tg2576+anti-GM-CSF antibody ($n = 5$)	8.3 ± 1.33			3.7 ± 0.9			0.8 ± 0.06			0.27 ± 1.5		

We found increased levels of soluble Aβ1-40 (23%, $P < 0.44$) and insoluble Aβ1-40 (27%, $P < 0.18$) in Tg2576 mice injected with anti-GM-CSF antibody compared with Tg2576 mice injected with PBS (control). However, these increased levels are not statistically significant may be because of small sample size ($n = 5$ in each group).
Interestingly, we also found decreased levels of soluble Aβ1-42 (46%, $P < 0.28$) in Tg2576 mice injected with anti-GM-CSF antibody compared with Tg2576 mice injected with PBS (control). However, these increased levels are not statistically significant.

Immunoglobulin isotyping revealed that the induced anti-Aβ antibodies were predominantly the IgG2b and IgG1 isotypes. They found decreased Aβ loads in the brain of the Tg2576 mice vaccinated with the adenovirus vectors encoding Aβ and GM-CSF compared with control Tg2576 mice. These studies, however, did not quantify the levels of Aβ1-42 and Aβ1-40 in the GM-CSF-treated Tg2576 mice.

DaSilva *et al*. (39) vaccinated APP mice with Aβ, GM-CSF and IL4 and found this combinational approach decreased Aβ plaque load by 43% in AD transgenic mice. Frazer *et al*. (47) used an adenoviral cassette (HSV(IE)Aβ(CMV)IL4) that co-delivered Aβ1-42 with an interleukin-4 in a triple-transgenic mice model. They found increased levels of Aβ-specific antibodies, improved learning and improved memory, and decreased AD pathological features in the vaccinated mice compared with the other experimental groups (47). In another study, using a gene-gun delivery approach, Qu *et al*. (78) delivered Aβ42 into double-transgenic (APPswe/PS1DeltaE9) mice and found that the vaccinated mice developed Th2 antibodies (IgG1) against Aβ42. The levels of Aβ42 in brain decreased by 41%, and the level of plasma increased by 43% in the vaccinated mice compared with the control mice. Similar to the Qu *et al*. (78) study, several other studies using AD transgenic mice (79) and non-human primate monkeys (80,81) found decreased levels of Aβ and ameliorated cognitive deficits in animals vaccinated with Aβ42. However, the long-term consequences of these Aβ immunizations are still unclear in clinical trials in which AD patients were vaccinated with Aβ. Findings from immunization human clinical trials using Aβ antibodies have not given positive results thus far other than decreasing Aβ deposits. Several laboratories using AD transgenic mice and non-human primates are currently studying the biochemistry of Aβ and the specificity of Aβ42 antibodies to decrease Aβ production.

We propose that anti-GM-CSF antibody may play a key role in decreasing the production of Aβ1-42 and the increasing of Aβ1-40 levels via blocking the γ-secretase activity at the epsilon site (Aβ42-43 position). This notion needs further investigation of anti-GM-CSF antibody in a large number of Tg2576 mice and also in other AD transgenic mice lines that overexpress human mutant APP in mice. In support of GM-CSF involvement in altering Aβ production, Volmar *et al*. (71) investigated human embryonic kidney cells expressing mutant APP and CD40. They found increased levels of Aβ in kidney cells overexpressing both APP and CD40. The GM-CSF antibodies reduce the CD40 ligand-induced production of Aβ in kidney cells expressing APPsw and CD40. Treatment of these cells with recombinant GM-CSF increased Aβ levels, indicating that GM-CSF antibody may affect Aβ production. However, our study is a step forward in determining the effects of GM-CSF in Aβ production in AD pathogenesis, finding that Aβ1-42 is decreased in Tg2576 mice injected with the anti-GM-CSF antibody and that the anti-GM-CSF antibody can suppress microglial activity and decrease toxic Aβ1-42.

CONCLUSIONS

The mechanistic link between microglial activation and mutant APP/Aβ in AD progression is not completely understood.

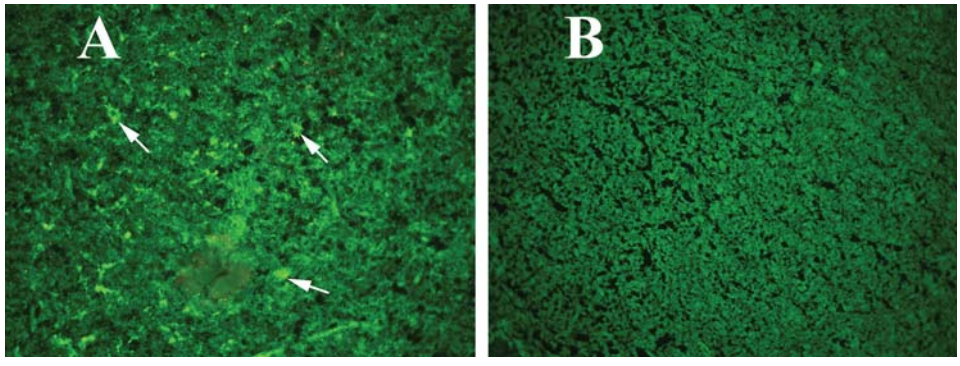

Figure 8. Immunoreactivity of IL6 in the cerebral cortex of a representative 10-month-old anti-GM-CSF antibody-injected Tg2576 mouse and a representative PBS vehicle-injected Tg2576 mouse. (**A**) Increased immunoreactivity of IL6 in a PBS vehicle-injected Tg2576 mouse and (**B**) decreased immunoreactivity of IL6 in an anti-GM-CSF antibody-injected (25 μg) Tg2576 mouse. Sections were photographed at ×40 the original magnification.

Further, the role of GM-CSF in activating pro-inflammatory cytokines in AD pathogenesis is still unclear. In the present study, we aimed to understand the connection between GM-CSF and microglial activity in AD progression. We investigated whether the anti-GM-CSF antibody can suppress microglial activity and decrease Aβ production in Tg2576 mice. We introduced the mouse GM-CSF antibody or PBS vehicle into the brains of 10-month-old male Tg2576 mice using ICV injections. We assessed the effect of several GM-CSF-associated pro-inflammatory cytokines on microglial activities and their association with Aβ using quantitative real-time RT–PCR, immunoblotting, immunohistochemistry and immunofluorescence analyses in anti-GM-CSF antibody-injected Tg2576 mice and PBS vehicle-injected control Tg2576 mice. Using sandwich ELISA technique, we measured intraneuronal Aβ in Tg2576 mice injected with GM-CSF antibody and PBS vehicle-injected control Tg2576 mice. Using double-labeling immunofluorescence analysis of intraneuronal Aβ, Aβ deposits and markers of microglia, and astrocytes, we assessed the relationship between intraneuronal Aβ and microglial markers, and Aβ deposits and pro-inflammatory cytokines in the Tg2576 mice injected with PBS vehicle and also in the anti-GM-CSF antibody-injected Tg2576 mice.

Our real-time RT–PCR analysis showed an increase in the mRNA expression of IL6, CD11c, IL1β, CD40 and CD11b in the cerebral cortices of the Tg2576 mice compared with their littermate non-transgenic controls. Immunohistochemistry findings of pro-inflammatory cytokines agreed with our real-time RT–PCR results. Interestingly, we found significantly decreased levels of activated microglia marked by CD11C, IL6 and CD40, and Aβ deposits in anti-GM-CSF antibody-injected Tg2576 mice compared with PBS vehicle-injected Tg2576 mice (negative controls). Findings from our real-time RT–PCR and immunoblotting analysis agreed with the immunohistochemistry observations. Our double-labeling analyses of intraneuronal Aβ and CD40 revealed that intraneuronal Aβ is associated with neuronal expression of CD40 in Tg2576 mice. Our quantitative sandwich ELISA analysis revealed that decreased levels of soluble Aβ1-42 and increased levels of Aβ1-40 in Tg2576 mice injected with the anti-GM-CSF antibody compared with Tg2576 mice injected with PBS vehicle, suggesting that anti-GM-CSF antibody decreases soluble Aβ1-42 production and suppresses microglial activity in Tg2576 mice. These findings indicating the ability of the anti-GM-CSF antibody to reduce Aβ1-42 and microglial activity in Tg2576 mice may have therapeutic implications for AD.

MATERIALS AND METHODS

Tg2576 mice

The Tg2576 mouse model was generated with the mutant human APP gene 695 amino acid isoform and with a double mutation ($Lys^{670}Asn$ and $Met^{671}Leu$) (82). This highly expressed human APP transgenic mice model exhibits an age-dependent appearance of Aβ plaques as well as a distribution of the Aβ plaque that is confined to the cerebral cortex and the hippocampus, sparing the striatum, the deep gray nuclei, and the brain stem. A correlation has been found between elevated amounts of soluble Aβ and increased free-radical production (10). This Tg2576 mouse model also parallels AD in that the Aβ plaques evoke a microglial reaction in their immediate vicinity.

Ten-month-old Tg2576 male mice (25–40 g) and age-matched, non-transgenic male littermates ('controls'; 25–40 g) were purchased from Taconic Farms (New York, NY, USA) and housed at the animal facility of the Oregon National Primate Center at Oregon Health and Science University (OHSU). We investigated 10-month-old Tg2576 mice ($n = 5$) and age-matched, non-transgenic littermates ($n = 5$) for mRNA abundance using quantitative RT–PCR and assessed Aβ deposits, microglia and astrocytes using immunohistochemistry. Further, using ICV injections, we injected anti-GM-CSF antibody into the brains of the Tg2576 mice ($n = 5$) and PBS vehicle into the brains of the Tg2576 mice ($n = 5$) as the 'negative control' and investigated mRNA abundance using quantitative RT–PCR, measured soluble and insoluble Aβ1-40 and Aβ1-42 using sandwich ELISA, and Aβ deposits, assessed microglia and astrocytes using immunohistochemistry. The OHSU Institutional Animal Care and Use Committee approved all procedures for animal care according to the guidelines set forth by NIH.

The anti-GM-CSF antibody

The anti-GM-CSF anti-mouse antibody (MP1-22E9, R &D Systems, Minneapolis, MN, USA) was supplied by KaloBios

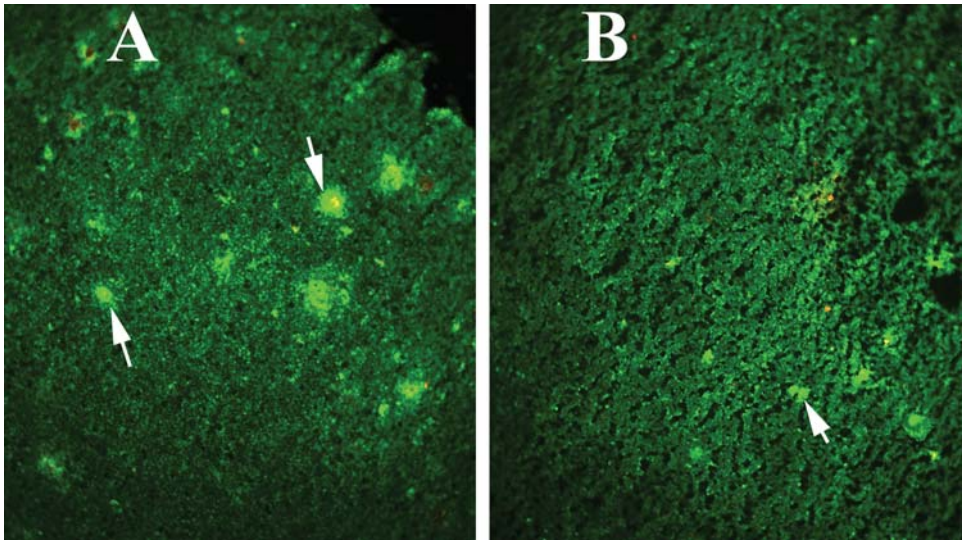

Figure 9. Immunoreactivity of CD11c in the cerebral cortex of a representative 10-month-old anti-GM-CSF antibody-injected Tg2576 mouse and a representative PBS vehicle-injected Tg2576 mouse. (**A**) Increased immunoreactivity of CD11c in a PBS vehicle-injected Tg2576 mouse and (**B**) decreased immunoreactivity of CD11c in an anti-GM-CSF antibody-injected (25 μg) Tg2576 mouse. Sections were photographed at ×40 the original magnification.

Pharmaceuticals (Palo Alto, CA, USA). This antibody was originally developed from a murine hybridoma derived from a rat treated with purified, recombinant mouse GM-CSF antigen.

The reagents for real-time RT–PCR

RNA isolation and cDNA synthesis reagents, including TriZol, reverse transcriptase superscript and other chemicals were purchased from Invitrogen (Carlsbad, CA, USA), and real-time RT–PCR reagents were purchased from Applied Biosystems (Foster City, CA, USA). Using Primer Express software (Applied Biosystems), we designed the oligonucleotide primers for the housekeeping genes, β-actin, GAPDH, mitochondrial encoded gene, NDAH-subunit 1, TNFα, IL1, IL6, gp91, CD11b, CD11c, CD40, CD45, MHCII-2, GFAP and NeuN. The primer sequences are as follows: TNFα: forward primer 5′-TT CGGCTACCCCAAGTTCAT-3′ and reverse primer 5′-CGCAC GTAGTTCCGCTTTC-3′; IL1β: forward primer 5′-CCATGGC ACATTCTGTTCAAA-3′ and reverse primer 5′-GCCCATC AGAGGCAAGGA-3′; IL6: forward primer 5′-CCACGGCC TTCCCTACTTC-3′ and reverse primer 5′-TTGGGAGTGGTA TCCTCTGTGA-3′; CD11b: forward primer 5′-AAACCACA GTCCCGCAGAGA-3′ and reverse primer 5′-CGTGTTCA CCAGCTGGCTTA-3′; CD11C: forward primer 5′-CCTG AGGGTGGGCTGGAT-3′ and reverse primer 5′-GCCAATTT CCTCCGGACAT-3′; CD40: forward primer 5′-TTCGAGT CAACGCCCATTC-3′ and reverse primer 5′-GATCCACTGCT GGGCTTCA-3′; CD45: forward primer 5′-GAACATGCTGCC AATGGTTCT-3′ and reverse primer 5′-TGTCCCACATGAC TCCTTTCC-3′; Gp91: forward primer 5′-CCCTCGGACTTT GGCAAA-3′ and reverse primer 5′-CCAGACTCGAGTATC GCTGACA-3′; MHCII-2: forward primer 5′-CTATGATGGCC GCGATTACA-3′ and reverse primer 5′-GCTGCTGTCCACG TTTTCAG-3′; GFAP: forward primer 5′-CCAGCTTCGAG CCAAGGA-3′ and reverse primer 5′-GAAGCTCCGCCTGG TAGACA-3′; NeuN: forward primer 5′-GGCAATGGTGGG ACTCAAAA-3′ and reverse primer 5′-GGGACCCGCTCCTT CAAC-3′; housekeeping genes: β-actin: forward primer 5′-AC GGCCAGGTCATCACTATTC-3′ and reverse primer 5′-AGG AAGGCTGGAAAAGAGCC-3′; NADH-subunit 1: forward primer 5′-CGGGCCCCCTTCGAC-3′ and reverse primer 5′-GG CCGGCTGCGTATTCT-3′; GAPDH: forward primer 5′-TT CCCGTTCAGCTCTGGG-3′ and reverse primer 5′-CCCTGC ATCCACTGGTGC-3′. The oligonucleotide real-time RT–PCR primers were synthesized and obtained from Invitrogen.

Reagents for immunohistochemistry and immunofluorescence analyses

Table 3 presents the immunochemicals, including primary and secondary antibodies and their dilutions, and other reagents used in the immunohistochemistry and immunofluorescence analyses of this study.

ICV injections

To inject the anti-GM-CSF mouse antibody, we performed survival surgeries for all mice. For the anti-GM-CSF antibody injections, the mice were anesthetized with 7% chloral hydrate (280 mg/kg) using intraperitoneal injections. The fur was shaved in the head area, and the mice were placed in a stereotactic apparatus with a mouse adaptor. A small burr hole was made in the skull overlying the lateral ventricle. Five to 7 μl of the anti-GM-CSF antibody (25 μg) or PBS vehicle was injected into the lateral ventricle through a 33 gauge injector attached to a 10 ml Hamilton syringe (Hamilton Co., Reno, NV, USA). Injections were given over the span of 5 min, after which the cannula was left in place for an additional 5 min to allow for diffusion. After the injection, the skin was closed with sutures or wound clips, and the wounds were treated with xylocaine and iodine. Mice were kept warm and carefully monitored during recovery from anesthesia, and

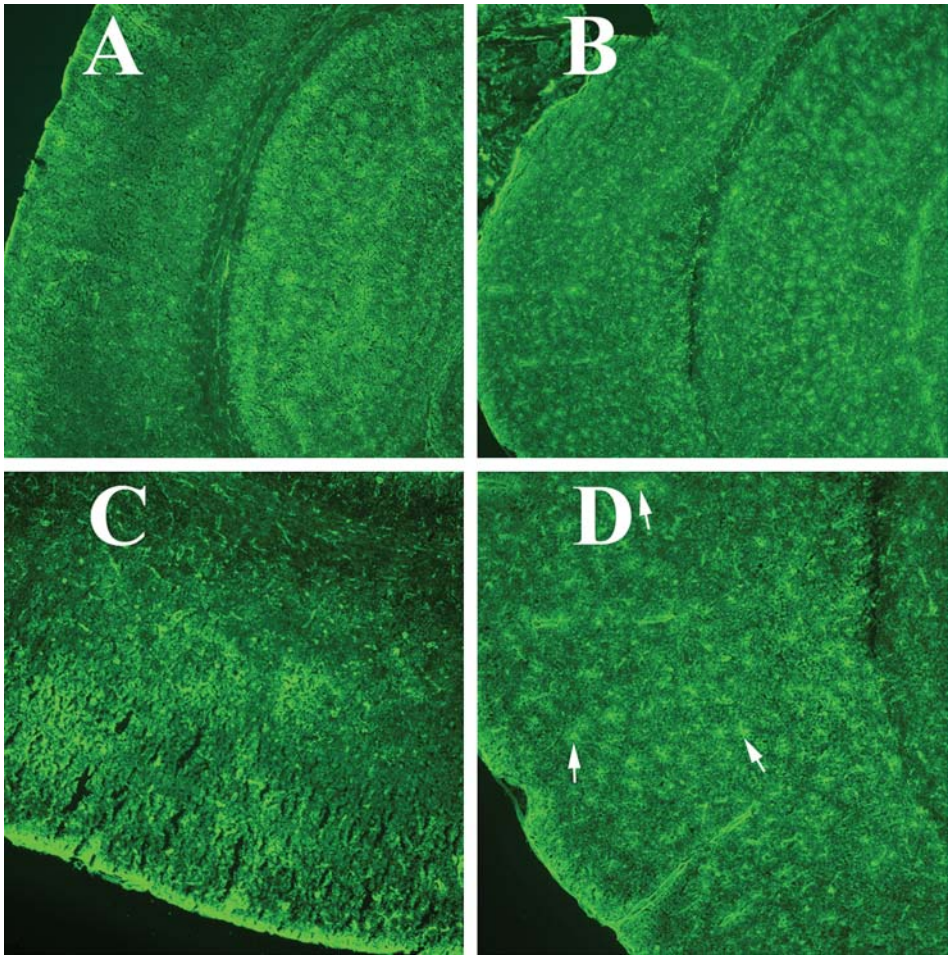

Figure 10. Immunoreactivity of GFAP in a representative 10-month-old anti-GM-CSF antibody-injected Tg2576 mouse and a representative PBS vehicle-injected Tg2576 mouse. (**A**) Immunoreactivity of GFAP in a PBS vehicle-injected Tg2576 mouse, (**B**) increased immunoreactivity of GFAP in the cerebral cortex and hippocampus of an anti-GM-CSF antibody-injected Tg2576 mouse, (**C**) GFAP immunoreactivity of cerebral cortex from a PBS vehicle-injected Tg2576 mouse and (**D**) increased immunoreactivity of cerebral cortex in an anti-GM-CSF antibody-injected Tg2576 mouse. (A) and (B) were photographed at $\times 5$ the original magnification, and (C) and (D) at $\times 20$.

then placed in individual cages. Five days after the ICV injections, the mice were re-anesthetized and sacrificed by cervical dislocation since maximum immunoreactivity of microglial markers was reported at 4–5 days after GM-CSF induction (83). The brains were collected from all mice and the cerebral cortex (from the front brain) and cerebellum were dissected from the brains separately. The soluble and insoluble Aβ levels were measured from cerebral cortex tissues. The midbrains (containing hippocampus, cerebral cortex and striatum) were dissected and flash-frozen. Sections with 10 μm-thickness were cut from the midbrain and used for immunohistochemistry of cytokines and Aβ deposits.

Quantification of mRNA expression of markers of microglia, astrocytes and neurons using real-time RT–PCR

Total RNA was isolated from dissected cerebral cortex tissues from each group of experimental and control group mice using the TriZol reagent (Invitrogen). As shown in Table 2, mRNA expression of several cytokines, GFAP and neuronal markers was measured using SYBR-Green chemistry-based quantitative real-time RT–PCR, as described by Manczak *et al*. (84). Briefly, 1 μg of DNAse-treated total RNA was used as starting material, to which were added 1 μl of oligo (dT), 1 μl of 10 mM dNTPs, 4 μl of 5× first-strand buffer, 4 μl of 25 mM $MgCl_2$, 2 μl of 0.1 M DTT and 1 μl of RNAse out. The reagents RNA, oligo (dT) and dNTPs were mixed first, heated at 65°C for 5 min and then chilled on ice until other components were added. The samples were incubated at 42°C for 2 min. Then 1 μl of Superscript II (40 U/μl) (Invitrogen) was added, and the samples were incubated at 42°C for 50 min. The reaction was inactivated by heating the contents at 70°C for 15 min.

Real-time quantitative PCR amplification reactions were carried out in an ABI Prism 7900 sequence detection system (Applied Biosystems) in a 25 μl volume of total reaction mixture. The reaction mixture consisted of 1× PCR buffer containing SYBR-Green; 3 mM $MgCl_2$; 100 nM of each primer; 200 nM each of dATP, dGTP and dCTP; 400 nM of

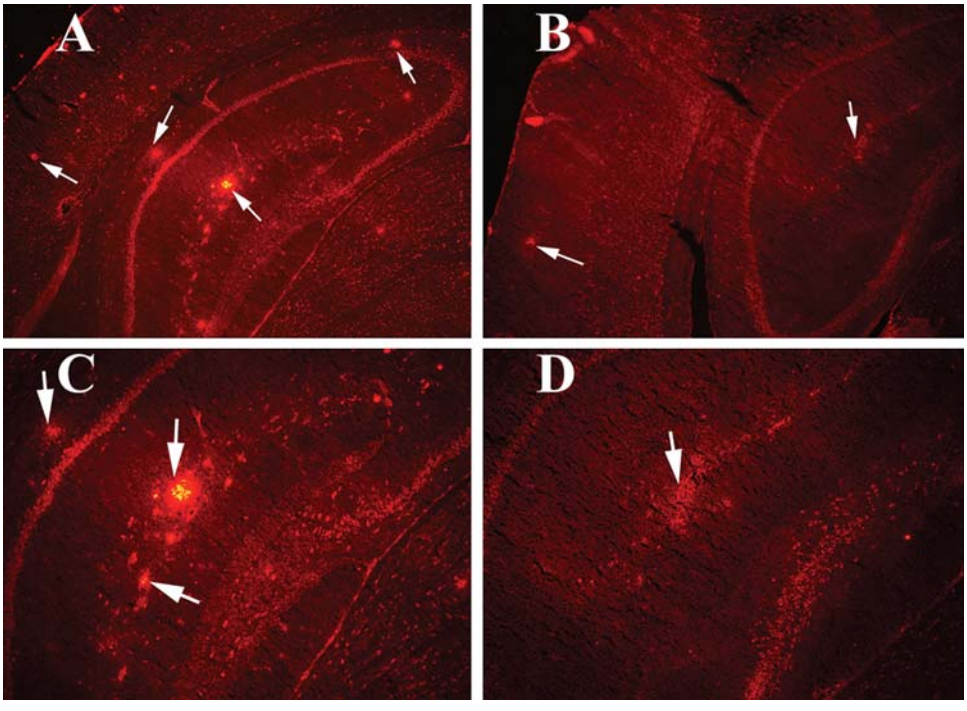

Figure 11. Immunoreactivity of Aβ deposits in a representative 10-month-old anti-GM-CSF antibody-injected Tg2576 mouse and a representative PBS vehicle-injected Tg2576 mouse. The E610 antibody recognized both intraneuronal Aβ and Aβ deposits in mouse brain sections. (**A**) Aβ deposits in the cerebral cortex and hippocampus of a PBS vehicle-injected Tg2576 mouse, (**B**) decreased Aβ deposits in the cerebral cortex and hippocampus in an anti-GM-CSF antibody-injected mouse, (**C**) Aβ deposits in the hippocampus of a PBS vehicle-injected Tg2576 mouse and (**D**) decreased Aβ deposits in the hippocampus of an anti-GM-CSF antibody-injected mouse. (A) and (B) were photographed at $\times 5$ the original magnification, and (C) and (D), at $\times 10$.

dUTP; 0.01 U/μl of AmpErase UNG and 0.05 U/μl of AmpliTaq Gold (ABI). Twenty nanograms of cDNA template was added to each reaction mixture.

To determine the unregulated endogenous reference gene in AD mice, the C_T values (cycle threshold values) of β-actin, GAPDH and NADH-subunit (mitochondrial-encoded gene) were tested. The C_T value was the cycle number at which the fluorescence generated within a reaction crosses the threshold within the linear phase of the amplification profile. The C_T value is an important quantitative parameter in real-time PCR analysis (84,85). All reactions were carried out in duplicate with a no-template control. The PCR conditions were 50°C for 2 min, 95°C for 10 min, followed by 40 cycles of 95°C for 15 s and 60°C for 1 min. The fluorescent spectra were recorded during the elongation phase of each PCR cycle. To distinguish specific amplicons from non-specific amplifications, a dissociation curve was generated. The C_T values were calculated with sequence-detection system software V1.7 (Applied Biosystems) and an automatic setting of baseline, which was the average value of PCR, cycles 3–15, plus C_T generated 10 times its standard deviation. The amplification plots and C_T values were exported from the exponential phase of PCR directly into a Microsoft Excel worksheet for further analysis.

The mRNA transcript level was normalized against β-actin, GAPDH and mitochondrial-encoded complex I gene—NADH-subunit 1 at each dilution. The standard curve was the normalized mRNA transcript level plotted against the log-value of the input cDNA concentration at each dilution. To compare β-actin, GAPDH and NADH-subunit 1 and cytokine markers, relative quantification was performed according to the CT method of ABI (84). Briefly, the comparative C_T method involved averaging duplicate samples taken as the C_T values for β-actin, GAPDH and NADH-subunit 1 and cytokine markers. We used β-actin normalization in the present study because β-actin C_T values are similar for PBS-injected Tg2576 mice, anti-GM-CSF-injected Tg2576 mice and the non-transgenic littermates (without the APP mutation). The ΔC_T value was obtained by subtracting the average β-actin C_T value from the average C_T value of cytokine markers. The present study used the average ΔC_T of five animals as the calibrator. The fold change was calculated according to the formula $2^{-(\Delta\Delta C_T)}$, where $\Delta\Delta C_T$ was the difference between ΔC_T and the ΔC_T calibrator value.

Immunoblotting analysis of microglial markers in Tg2576 mice injected with PBS-vehicle and GM-CSF antibody-injected Tg2576 mice

To determine whether GM-CSF antibody suppressed the protein levels of microglial markers that showed decreased mRNA expression in our real-time RT–PCR in Tg2576 mice injected with GM-CSF antibody, we studied immunoblotting analysis of protein lysates from Tg2576 mice injected with GM-CSF antibody and Tg2576 mice injected with PBS vehicle. Twenty micrograms of protein lysate from cerebral cortex was resolved on 12% SDS–PAGE, and the resolved proteins were transferred to nylon membranes (Novax Inc., San Diego, CA, USA) that were then incubated at room temperature with a blocking buffer (5% dry milk dissolved in a

Table 3. Summary of antibody dilutions and conditions used in the immunohistochemistry/immunofluorescence analyses of cytokine markers and Aβ deposits in PBS vehicle-injected Tg2576 mice and anti-GM-CSF antibody-injected Tg256 mice

Marker	Primary antibody: species and dilution	Supplier	Secondary antibody, dilution, Alexa dye	Supplier
Aβ	Mouse monoclonal 1:300	Covance, San Diego, CA, USA	Goat-anti mouseAlexa594	Molecular Probes, Eugene, OR, USA
TNFα	Rabbit polyclonal 1:200	Abcam, Cambridge, MA, USA	Goat anti-rabbit HRP 1:400	KPL, Gaithersburg, MD, USA
			TSA-Alexa488	Molecular Probes, Eugene, OR, USA
IL1β	Rabbit polyclonal 1:100	Abcam, Cambridge, MA, USA	Goat anti-rabbit HRP 1:400	KPL, Gaithersburg, MD, USA
			TSA-Alexa488	Molecular Probes, Eugene, OR, USA
IL6	Rabbit polyclonal 1:400	Abcam, Cambridge, MA, USA	Goat anti-rabbit HRP 1:400	KPL, Gaithersburg, MD, USA
			TSA-Alexa488	Molecular Probes, Eugene, OR, USA
CD11b	Rat monoclonal 1:100	Abcam, Cambridge, MA, USA	Goat anti-rat biotin 1:300	KPL, Gaithersburg, MD, USA
			ABC	VECTOR, Invitrogen, Carlsbad, CA, USA
			TSA-Alexa488	Molecular Probes, Eugene, OR, USA
CD11c	Hamster monoclonal 1:50	Chemicon-Millipore, Temecula, CA, USA	Goat anti-hamster biotin 1:300	KPL, Gaithersburg, MD, USA
			ABC	VECTOR, Invitrogen, Carlsbad, CA, USA
			TSA-Alexa488	Molecular Probes, Eugene, OR, USA
CD40	Rabbit polyclonal 1: 100	Abcam, Cambridge, MA, USA	Goat anti-rabbit HRP 1:400	KPL, Gaithersburg, MD, USA
			TSA-Alexa488	Molecular Probes, Eugene, OR, USA
GFAP	Rabbit polyclonal 1:400	DakoCytomation,Carpinteria, CA, USA	Goat anti-rabbit HRP 1:400	KPL,Gaithersburg, MD, USA
			TSA-Alexa488	Molecular Probes, Eugene, OR, USA
NeuN	Mouse Monoclonal 1:200	Chemicon-Millipore, Temecula, CA, USA	Goat anti-mouse HRP 1:400	KPL, Gaithersburg, MD, USA
			TSA-Alexa488	Molecular Probes, Eugene, OR, USA

TBST buffer) for 1 h. The nylon membranes were incubated overnight with the primary antibodies CD11b (1:500) (rat-monoclonal; Abcam, Cambridge, MA, USA), CD40 (1:200) (rabbit-polyclonal), IL1β (1:500) (rabbit-polyclonal), IL6 (1:500) (rabbit-polyclonal) and β-actin (1:500) (mouse-monoclonal; Chemican-Millipore, Temicula, CA, USA). The membranes were washed with a TBST buffer three times at 10 min intervals and then incubated with appropriate secondary antibodies (for IL1β, donkey anti-rabbit 1:15,000; Il6, donkey-anti-rabbit 1:15,000; CD11b, goat anti-rat 1:8000; CD40, donkey anti-rabbit; β-actin, sheep-anti-mouse 1:10,000) for 2 h, followed by washing again three times with a TBST buffer. Microglial proteins were detected with chemiluminescent reagents (Pierce Biotechnology) and the bands from immunoblots were quantified on a Kodak Scanner (ID Image Analysis Software, Kodak Digital Science, Kennesaw, GA, USA). Briefly, ID image analysis was used to analyze gel images captured with a Kodak Digital Science CD40 camera. The lanes were marked to define the positions and specific regions of the bands. ID's fine band command was used to locate the bands in each lane, to scan the bands and to record the readings.

Immunohistochemistry and immunofluorescence analyses of markers of microglia

To determine microglial activity, we used immunohistochemistry and immunofluorescence analyses of several selective cytokine markers that differentially expressed Tg276 mice relative to non-transgenic littermates, and anti-GM-CSF antibody-injected Tg2576 mice relative to the PBS-injected Tg2576 mice of our real-time RT–PCR assay. Briefly, we fixed the fresh-frozen midbrain sections (covering hippocampus and cortex) from these mice by dipping into a 4% paraformaldehyde solution for 10 min at room temperature. The sections were incubated overnight at room temperature with cytokine antibodies (Table 3) according to the recommended dilutions by manufacturers. The next day, the sections were incubated with the secondary antibody conjugated with HRP or biotin-labeled secondary antibody (see Table 3 dilutions) for 1 h, and further sections were incubated with tyramide-labeled or streptoavidin-conjugated fluorescent dye, Alexa 594 (red) or Alexa 488 (green) (Molecular Probes, Eugene, OR, USA). Photographs were taken using a fluorescence microscope.

To quantify the immunoreactivity of microglial markers IL1β, IL6, CD40 and CD11c, for each animal three to four sections of the midbrain covering hippocampus and cortex were stained as described earlier and quantified as follows: from immunostained sections, several photographs were taken at $\times 20$ (the original) magnification covering 80–90% of cortex and hippocampus (amyloid-rich regions) of the brain. Positive immunoreactive fluorescence signal intensity of microglia was measured using red-green and blue (RGB) method (86). We quantified the signal intensity of immunoreactivity for several randomly selected images for each animal and assessed statistical significance using a Student's *t*-test for each microglial marker between PBS vehicle-injected Tg2576 mice and Tg2576 mice injected with GM-CSF antibody.

Immunohistochemistry and immunofluorescence analyses of Aβ deposits

To determine the Aβ deposits in the PBS-injected Tg2576 mice and anti-GM-CSF antibody-injected Tg2576 mice, we

used immunohistochemistry and immunofluorescence analyses, as described in Manczak *et al*. (10). Briefly, we fixed the midbrain sections and incubated them overnight at room temperature with a mouse anti-human Aβ antibody, E610 (see Table 3 for dilutions). The next day, the sections were incubated with the goat anti-mouse secondary antibody conjugated with fluorescent dye Alexa 594 (red) (Molecular Probes) for 1 h at room temperature. Photographs were taken with a fluorescence microscope.

To quantify the immunoreactivity of Aβ deposits, for each animal three to four sections of the midbrain covering hippocampus and cortex were stained as described earlier and used for quantification purpose. From these sections, several photographs were taken at ×20 magnification covering 80–90% of cortex and hippocampus (amyloid-rich regions) of the brain. Positive immunoreactive fluorescence signal intensity of Aβ deposits was measured using RGB method (86). We quantified the signal intensity of immunoreactivity for several randomly selected images for each animal and assessed statistical significance using a Student's *t*-test for Aβ deposits between PBS vehicle-injected Tg2576 mice and Tg2576 mice injected with GM-CSF antibody.

Double-labeling analysis of intraneuronal Aβ and Aβ deposits and markers of microglia

To determine the precise connection between intraneuronal Aβ and Aβ deposits and microglia, we performed double-labeling immunohistochemistry and immunofluorescence analyses using a mouse anti-human Aβ antibody, E610, and antibodies of markers of microglia IL1β, IL6, CD11b, CD11c, CD40 and GFAP as described in Manczak *et al*. (10). Briefly, we fixed the midbrain sections and incubated them overnight at room temperature with a mouse anti-human Aβ antibody (see Table 3 for dilutions). The next day, the sections were incubated with the secondary antibody conjugated with the fluorescent dye Alexa 594 (red) (Molecular Probes) for 1 h at room temperature. For the second labeling, the sections were incubated overnight with primary antibodies of cytokines, IL1β, IL6, CD11b, CD11c, CD40 and GFAP (see Table 3 for dilutions). On the third day, for cytokines, the sections were incubated with biotin-labeled secondary antibody for 30 min, ABC complex for another 30 min and tyramide-labeled fluorescent dye Alexa 488 (green) for 10 min.

For GFAP, the sections were incubated with a secondary antibody conjugated with HRP for 1 h at room temperature. Finally, the slides were incubated with tyramide-labeled Alexa 488 the (green). Photographs were taken with a fluorescence microscope.

Double-labeling analysis of CD40 and neuronal marker, NeuN

To determine whether CD40 is expressed in neurons, we performed double-labeling immunohistochemistry and immunofluorescence analyses using rabbit anti-CD40 antibody and mouse anti-neuronal marker NeuN. We fixed the midbrain sections and incubated them overnight at room temperature with rabbit anti-CD40 antibody (see Table 3 for dilutions). The next day, the sections were incubated with the biotin-labeled secondary antibody for 30 min, next with ABC complex for another 30 min and finally with the tyramide-labeled fluorescent dye Alexa 594 (red) (Molecular Probes) for 10 min at room temperature. For the second labeling, the sections were incubated overnight with mouse anti-NeuN antibody (see Table 3 for dilutions). On the third day, the sections were incubated with secondary antibody conjugated with HRP for 1 h at room temperature. Finally, the slides were incubated with the tyramide-labeled fluorescent dye Alexa 488 (green). Photographs were taken with a fluorescence microscope.

Measurement of soluble and insoluble Aβ levels using sandwich ELISA

To determine whether the anti-GM-CSF antibody decreases soluble and insoluble Aβ levels in Tg2576 mice, we measured soluble and insoluble Aβ levels in PBS-injected Tg2576 mice and anti-GM-CSF antibody-injected Tg2576 mice as described in Manczak *et al*. (10). Briefly, cerebral cortex tissues were homogenized in Tris-buffered saline, pH 8.0, containing protease inhibitors (20 mg/ml pepstatin A, aprotinin, phosphsoramidon and leupeptin; 0.5 mM PMSF; 1 mM EGTA). Samples were sonicated briefly and centrifuged at 10 000*g* for 20 min at 4°C. Using ELISA, we determined the soluble Aβ fraction. To measure the insoluble Aβ, we re-suspended the pellet in 70% formic acid and again centrifuged the pellet. The extract was neutralized with 0.25 M Tris, pH 8.0, containing 30% acetonitrile and 5 M NaOH before we determined the insoluble Aβ using ELISA. For each sample, we measured Aβ1-40 and Aβ1-42 using commercial colorimetric ELISA kits (Biosource International, Camarillo, CA, USA), specific for each species. A 96-well plate washer and reader were used, according to the manufacturer's instructions. Each sample was run in duplicate. The protein concentration of the homogenates was determined by the BCA method, and Aβ was expressed as picogram of Aβ per milligram protein.

Statistical considerations

Statistical analyses were conducted for soluble and insoluble Aβ, in both treated and untreated Tg2576 mice with anti-GM-CSF antibody using a Student's *t*-test. We also quantified the immunoreactivity of microglial markers IL1β, IL6, CD40 and CD11c between Tg2576 mice and Tg2576 mice injected with GM-CSF antibody. For each microglial marker, we assessed the statistical significance using a Student's *t*-test. The statistical significance of Aβ deposits between Tg2576 mice and Tg2576 mice injected with GM-CSF antibody was assessed using a Student's *t*-test.

SUPPLEMENTARY MATERIAL

Supplementary Material is available at *HMG* online.

ACKNOWLEDGEMENTS

We thank Dr Shaun Morrison for allowing us to use the stereotaxic apparatus for GM-CSF experiments conducted for this

study. We thank the scientists of KaloBios and Drs Geoffrey Yarranton and Varghese Palath for their constructive comments on the manuscript.

Conflict of Interest statement. None declared.

FUNDING

The research presented in this paper was supported by KaloBios Pharmaceuticals via OHSU-Technology Research Collaborations Research Agreement and NIH grants (AG028072, AG026051 and RR00163).

REFERENCES

1. Selkoe, D.J. (2001) Alzheimer's disease: genes, proteins, and therapy. *Physiol. Rev.*, **81**, 741–766.
2. Mattson, M.P. (2004) Pathways towards and away from Alzheimer's disease. *Nature*, **430**, 631–639.
3. Wyss-Coray, T. (2006) Inflammation in Alzheimer disease: driving force, bystander or beneficial response? *Nat. Med.*, **12**, 1005–1015.
4. LaFerla, F.M., Green, K.N. and Oddo, S. (2007) Intracellular amyloid-beta in Alzheimer's disease. *Nat. Rev. Neurosci.*, **8**, 499–509.
5. Reddy, P.H. and Beal, M.F. (2008) Amyloid beta, mitochondrial dysfunction and synaptic damage: implications for cognitive decline in aging and Alzheimer's disease. *Trends Mol. Med.*, **14**, 45–53.
6. Selkoe, D.J. (2002) Alzheimer's disease is a synaptic failure. *Science*, **298**, 789–791.
7. Reddy, P.H., Mani, G., Park, B.S., Jacques, J., Murdoch, G., Whetsell, W. Jr, Kaye, J. and Manczak, M. (2005) Differential loss of synaptic proteins in Alzheimer's disease: implications for synaptic dysfunction. *J. Alzheimers Dis.*, **7**, 103–117.
8. Reddy, P.H. and McWeeney, S. (2006) Mapping cellular transcriptosomes in autopsied Alzheimer's disease subjects and relevant animal models. *Neurobiol. Aging*, **27**, 1060–1077.
9. Reddy, P.H., McWeeney, S., Park, B.S., Manczak, M., Gutala, R.V., Partovi, D., Jung, Y., Yau, V., Searles, R., Mori, M. and Quinn, J. (2004) Gene expression profiles of transcripts in amyloid precursor protein transgenic mice: upregulation of mitochondrial metabolism and apoptotic genes is an early cellular change in Alzheimer's disease. *Hum. Mol. Genet.*, **13**, 1250–1240.
10. Manczak, M., Anekonda, T.S., Henson, E., Park, B.S., Quinn, J. and Reddy, P.H. (2006) Mitochondria are a direct site of Abeta accumulation in Alzheimer's disease neurons: implications for free radical generation and oxidative damage in disease progression. *Hum. Mol. Genet.*, **15**, 1437–1449.
11. Devi, L., Prabhu, B.M., Galati, D.F., Avadhani, N.G. and Anandatheerthavarada, H.K. (2006) Accumulation of amyloid precursor protein in the mitochondrial import channels of human Alzheimer's disease brain is associated with mitochondrial dysfunction. *J. Neurosci.*, **26**, 9057–9068.
12. Mattson, M.P., Gleichmann, M. and Cheng, A. (2008) Mitochondria in neuroplasticity and neurological disorders. *Neuron*, **60**, 748–766.
13. Reddy, P.H. (2008) Mitochondrial medicine for aging and neurodegenerative diseases. *Neuromolecular Med.*, **10**, 291–315.
14. McGeer, E.G. and McGeer, P.L. (2003) Inflammatory processes in Alzheimer's disease. *Prog. Neuropsychopharmacol. Biol. Psychiatry*, **27**, 741–749.
15. Mehlhorn, G., Hollborn, M. and Schliebs, R. (2000) Induction of cytokines in glial cells surrounding cortical beta-amyloid plaques in transgenic Tg2576 mice with Alzheimer pathology. *Int. J. Dev. Neurosci.*, **18**, 423–431.
16. Apelt, J. and Schliebs, R. (2001) Beta-amyloid-induced glial expression of both pro- and anti-inflammatory cytokines in cerebral cortex of aged transgenic Tg2576 mice with Alzheimer plaque pathology. *Brain Res.*, **891**, 21–30.
17. Abbas, N., Bednar, I., Mix, E., Marie, S., Paterson, D., Ljungberg, A., Morris, C., Winblad, B., Nordberg, A. and Zhu, J. (2002) Up-regulation of the inflammatory cytokines IFN-gamma and IL-12 and down-regulation of IL-4 in cerebral cortex regions of APP(SWE) transgenic mice. *J. Neuroimmunol.*, **126**, 50–57.
18. Li, R., Huang, Y.G., Fang, D. and Le, W.D. (2004) (-)-Epigallocatechin gallate inhibits lipopolysaccharide-induced microglial activation and protects against inflammation-mediated dopaminergic neuronal injury. *J. Neurosci. Res.*, **78**, 723–731.
19. Strohmeyer, R. and Rogers, J. (2001) Molecular and cellular mediators of Alzheimer's disease inflammation. *J. Alzheimer's Dis.*, **3**, 131–157.
20. Wirths, O., Breyhan, H., Marcello, A., Cotel, M.C., Brück, W. and Bayer, T.A. (2008) Inflammatory changes are tightly associated with neurodegeneration in the brain and spinal cord of the APP/PS1KI mouse model of Alzheimer's disease. *Neurobiol. Aging*, in press.
21. Banati, R.B. and Beyreuther, K. (1995) Alzheimer's disease. In Kettenma, H. and Ransom, B.R. (eds), *Neuroglia*, Oxford University Press, New York/Oxford, pp. 1027–1043.
22. Matsuoka, Y., Picciano, M., La Francois, J. and Duff, K. (2001) Fibrillar beta-amyloid evokes oxidative damage in a transgenic mouse model of Alzheimer's disease. *Neuroscience*, **104**, 609–613.
23. Maier, M., Peng, Y., Jiang, L., Seabrook, T.J., Carroll, M.C. and Lemere, C.A. (2008) Complement C3 deficiency leads to accelerated amyloid beta plaque deposition and neurodegeneration and modulation of the microglia/macrophage phenotype in amyloid precursor protein transgenic mice. *J. Neurosci.*, **28**, 6333–6341.
24. Tarkowski, E., Wallin, A., Regland, B., Blennow, K. and Tarkowski, A. (2001) Local and systemic GM-CSF increase in Alzheimer's disease and vascular dementia. *Acta Neurol. Scand.*, **103**, 166–174.
25. Tarkowski, E., Andreasen, N., Tarkowski, A. and Blennow, K. (2003) Intrathecal inflammation precedes development of Alzheimer's disease. *J. Neurol. Neurosurg. Psychiatry*, **74**, 1200–1205.
26. Frautschy, S.A., Yang, F., Irrizarry, M., Hyman, B., Saido, T.C., Hsiao, K. and Cole, G.M. (1998) Microglial response to amyloid plaques in APPsw transgenic mice. *Am. J. Pathol.*, **152**, 307–317.
27. Stalder, M., Phinney, A., Probst, A., Sommer, B., Staufenbiel, M. and Jucker, M. (1999) Association of microglia with amyloid plaques in brains of APP23 transgenic mice. *Am. J. Pathol.*, **154**, 1673–1684.
28. Wegiel, J., Wang, K.C., Imaki, H., Rubenstein, R., Wronska, A., Osuchowski, M., Lipinski, W.J., Walker, L.C. and LeVine, H. (2001) The role of microglial cells and astrocytes in fibrillar plaque evolution in transgenic APP(SW) mice. *Neurobiol. Aging*, **22**, 49–61.
29. Lim, G.P., Yang, F., Chu, T., Chen, P., Beech, W., Teter, B., Tran, T., Ubeda, O., Ashe, K.H., Frautschy, S.A. and Cole, G.M. (2000) Ibuprofen suppresses plaque pathology and inflammation in a mouse model for Alzheimer's disease. *J. Neurosci.*, **20**, 5709–5714.
30. Yan, Q., Zhang, J., Liu, H., Babu-Khan, S., Vassar, R., Biere, A.L., Citron, M. and Landreth, G. (2003) Anti-inflammatory drug therapy alters beta-amyloid processing and deposition in an animal model of Alzheimer's disease. *J. Neurosci.*, **23**, 7504–7509.
31. Itagaki, S., McGeer, P.L., Akiyama, H., Zhu, S. and Selkoe, D. (1989) Relationship of microglia and astrocytes to amyloid deposits of Alzheimer disease. *J. Neuroimmunol.*, **24**, 173–182.
32. Mattiace, L.A., Davies, P., Yen, S.H. and Dickson, D.W. (1990) Microglia in cerebellar plaques in Alzheimer's disease. *Acta Neuropathol. (Berl.)*, **80**, 493–498.
33. Sturchler-Pierrat, C., Abramowski, D., Duke, M., Wiederhold, K.H., Mistl, C., Rothacher, S., Ledermann, B., Bürki, K., Frey, P., Paganetti, P.A. *et al.* (1997) Two amyloid precursor protein transgenic mouse models with Alzheimer disease-like pathology. *Proc. Natl Acad. Sci. USA*, **94**, 13287–13292.
34. Gehrmann, J., Matsumoto, Y. and Kreutzberg, G.W. (1995) Microglia: intrinsic immuneffector cell of the brain. *Brain Res. Brain Res. Rev.*, **20**, 269–287.
35. Chao, C.C., Hu, S., Molitor, T.W., Shaskan, E.G. and Peterson, P.K. (1992) Activated microglia mediate neuronal cell injury via a nitric oxide mechanism. *J. Immunol.*, **149**, 2736–2741.
36. McGeer, P.L., Itagaki, S., Tago, H. and McGeer, E.G. (1987) Reactive microglia in patients with senile dementia of the Alzheimer type are positive for the histocompatibility glycoprotein HLA-DR. *Neurosci Lett.*, **79**, 195–200.
37. Rasko, J.E. and Gough, N.M. (1994) Granulocyte–macrocyte colony stimulating factor. In Thomson, A.W. (ed.), *The Cytokine Handbook*, 2nd edn. Academic Press, London. pp. 343–369.

38. Giulian, D., Li, J., Li, X., George, J. and Rutecki, P.A. (1994) The impact of microglia-derived cytokines upon gliosis in the CNS. *Dev. Neurosci.*, **16**, 128–136.
39. DaSilva, K., Brown, M.E., Westaway, D. and McLaurin, J. (2006) Immunization with amyloid-beta using GM-CSF and IL-4 reduces amyloid burden and alters plaque morphology. *Neurobiol. Dis.*, **23**, 433–444.
40. Zaheer, A., Zaheer, S., Sahu, S.K., Knight, S., Khosravi, H., Mathur, S.N. and Lim, R. (2007) A novel role of glia maturation factor: induction of granulocyte–macrophage colony-stimulating factor and pro-inflammatory cytokines. *J. Neurochem.*, **101**, 364–376.
41. Reddy, P.H., Manczak, M., Zhao, W., Nakamura, K., Mao, P., Bebbington, C.R., Yarranton, G.T. and Map, P. (2009) Granulocyte–macrophage colony-stimulating factor antibody suppresses microglial activity: implications for anti-inflammatory effects in Alzheimer's disease and multiple sclerosis. *J. Neurochem.*, in press.
42. Billings, L.M., Oddo, S., Green, K.N., McGaugh, J.L. and LaFerla, F.M. (2005) Intraneuronal Abeta causes the onset of early Alzheimer's disease-related cognitive deficits in transgenic mice. *Neuron*, **45**, 675–688.
43. Schroeter, S., Khan, K., Barbour, R., Doan, M., Chen, M., Guido, T., Gill, D., Basi, G., Schenk, D., Seubert, P. and Games, D. (2008) Immunotherapy reduces vascular amyloid-beta in PDAPP mice. *J. Neurosci.*, **28**, 6787–6793.
44. Tucker, S.M., Borchelt, D.R. and Troncoso, J.C. (2008) Limited clearance of pre-existing amyloid plaques after intracerebral injection of Abeta antibodies in two mouse models of Alzheimer disease. *J. Neuropathol. Exp. Neurol.*, **67**, 30–40.
45. Gardberg, A.S., Dice, L.T., Ou, S., Rich, R.L., Helmbrecht, E., Ko, J., Wetzel, R., Myszka, D.G., Patterson, P.H. and Dealwis, C. (2007) Molecular basis for passive immunotherapy of Alzheimer's disease. *Proc. Natl Acad. Sci. USA*, **104**, 15659–15664.
46. Kim, H.D., Kong, F.K., Cao, Y., Lewis, T.L., Kim, H., Tang, D.C. and Fukuchi, K. (2004) Immunization of Alzheimer model mice with adenovirus vectors encoding amyloid beta-protein and GM-CSF reduces amyloid load in the brain. *Neurosci. Lett.*, **370**, 218–223.
47. Frazer, M.E., Hughes, J.E., Mastrangelo, M.A., Tibbens, J.L., Federoff, H.J. and Bowers, W.J. (2008) Reduced pathology and improved behavioral performance in Alzheimer's disease mice vaccinated with HSV amplicons expressing amyloid-beta and interleukin-4. *Mol. Ther.*, **16**, 845–853.
48. Ravaglia, G., Forti, P., Maioli, F., Chiappelli, M., Montesi, F., Tumini, E., Mariani, E., Licastro, F. and Patterson, C. (2007) Blood inflammatory markers and risk of dementia: The Conselice Study of Brain Aging. *Neurobiol. Aging*, **28**, 1810–1820.
49. Lukiw, W.J. (2004) Gene expression profiling in fetal, aged, and Alzheimer hippocampus: a continuum of stress-related signaling. *Neurochem. Res.*, **29**, 1287–1297.
50. Papassotiropoulos, A., Hock, C. and Nitsch, R.M. (2001) Genetics of interleukin 6: implications for Alzheimer's disease. *Neurobiol. Aging*, **22**, 863–871.
51. Baron, R., Nemirovsky, A., Harpaz, I., Cohen, H., Owens, T. and Monsonego, A. (2008) IFN-gamma enhances neurogenesis in wild-type mice and in a mouse model of Alzheimer's disease. *FASEB J.*, **22**, 2843–2852.
52. Fan, R., Xu, F., Previti, M.L., Davis, J., Grande, A.M., Robinson, J.K. and Van Nostrand, W.E. (2007) Minocycline reduces microglial activation and improves behavioral deficits in a transgenic model of cerebral microvascular amyloid. *J. Neurosci.*, **27**, 3057–3063.
53. Burgess, B.L., McIsaac, S.A., Naus, K.E., Chan, J.Y., Tansley, G.H., Yang, J., Miao, F., Ross, C.J., van Eck, M., Hayden, M.R. *et al.* (2006) Elevated plasma triglyceride levels precede amyloid deposition in Alzheimer's disease mouse models with abundant A beta in plasma. *Neurobiol. Dis.*, **24**, 114–127.
54. Heneka, M.T., Sastre, M., Dumitrescu-Ozimek, L., Dewachter, I., Walter, J., Klockgether, T. and Van Leuven, F. (2005) Focal glial activation coincides with increased BACE1 activation and precedes amyloid plaque deposition in APP[V717I] transgenic mice. *J. Neuroinflammation*, **2**, 22.
55. Lee, J., Chan, S.L. and Mattson, M.P. (2002) Adverse effect of a presenilin-1 mutation in microglia results in enhanced nitric oxide and inflammatory cytokine responses to immune challenge in the brain. *Neuromolecular Med.*, **2**, 29–45.
56. Tehranian, R., Hasanvan, H., Iverfeldt, K., Post, C. and Schultzberg, M. (2001) Early induction of interleukin-6 mRNA in the hippocampus and cortex of APPsw transgenic mice Tg2576. *Neurosci. Lett.*, **301**, 54–58.
57. McGeer, P.L., McGeer, E.G. and Yasojima, K. (2000) Alzheimer disease and neuroinflammation. *J. Neural. Transm.*, **59** (suppl), 53–57.
58. Ryu, J.K. and McLarnon, J.G. (2008) A leaky blood-brain barrier, fibrinogen infiltration and microglial reactivity in inflamed Alzheimer's disease brain. *J. Cell. Mol. Med.*, in press.
59. Dudal, S., Krzywkowski, P., Paquette, J., Morissette, C., Lacombe, D., Tremblay, P. and Gervais, F. (2004) Inflammation occurs early during the Abeta deposition process in TgCRND8 mice. *Neurobiol. Aging*, **25**, 861–871.
60. Jana, M., Palencia, C.A. and Pahan, K. (2008) Fibrillar amyloid-beta peptides activate microglia via TLR2: implications for Alzheimer's disease. *J. Immunol.*, **181**, 7254–7262.
61. Zou, C.G., Zhao, Y.S., Gao, S.Y., Li, S.D., Cao, X.Z., Zhang, M. and Zhang, K.Q. (2009) Homocysteine promotes proliferation and activation of microglia. *Neurobiol. Aging*., in press.
62. Akiyama, H. and McGeer, P.L. (1990) Brain microglia constitutively express beta-2 integrins. *J. Neuroimmunol.*, **30**, 81–93.
63. Sasaki, A., Nakazato, Y., Ogawa, A. and Sugihara, S. (1996) The immunophenotype of perivascular cells in the human brain. *Pathol. Int.*, **46**, 15–23.
64. Town, T., Laouar, Y., Pittenger, C., Mori, T., Szekely, C.A., Tan, J., Duman, R.S. and Flavell, R.A. (2008) Blocking TGF-beta-Smad2/3 innate immune signaling mitigates Alzheimer-like pathology. *Nat. Med.*, **14**, 681–687.
65. Butovsky, O., Koronyo-Hamaoui, M., Kunis, G., Ophir, E., Landa, G., Cohen, H. and Schwartz, M. (2006) Glatiramer acetate fights against Alzheimer's disease by inducing dendritic-like microglia expressing insulin-like growth factor 1. *Proc. Natl Acad. Sci. USA*, **103**, 11784–11789.
66. de Groot, C.J., Hulshof, S., Hoozemans, J.J. and Veerhuis, R. (2001) Establishment of microglial cell cultures derived from postmortem human adult brain tissue: immunophenotypical and functional characterization. *Microsc. Res. Tech.*, **54**, 34–39.
67. Hallegua, D.S. and Weisman, M.H. (2002) Potential therapeutic uses of interleukin 1 receptor antagonists in human diseases. *Ann. Rheum. Dis.*, **61**, 960–967.
68. Guillemin, G.J., Williams, K.R., Smith, D.G., Smythe, G.A., Croitoru-Lamoury, J. and Brew, B.J. (2003) Quinolinic acid in the pathogenesis of Alzheimer's disease. *Adv. Exp. Med. Biol.*, **527**, 167–176.
69. Combs, C.K., Karlo, J.C., Kao, S.C. and Landreth, G.E. (2001) Beta-amyloid stimulation of microglia and monocytes results in TNFalpha-dependent expression of inducible nitric oxide synthase and neuronal apoptosis. *J. Neurosci.*, **21**, 1179–1188.
70. Buchhave, P., Janciauskiene, S., Zetterberg, H., Blennow, K., Minthon, L. and Hansson, O. (2009) Elevated plasma levels of soluble CD40 in incipient Alzheimer's disease. *Neurosci. Lett.*, **450**, 56–59.
71. Volmar, C.H., Ait-Ghezala, G., Frieling, J., Paris, D. and Mullan, M.J. (2008) The granulocyte macrophage colony stimulating factor (GM-CSF) regulates amyloid beta (Abeta) production. *Cytokine*, **42**, 336–344.
72. Ait-ghezala, G., Abdullah, L., Volmar, C.H., Paris, D., Luis, C.A., Quadros, A., Mouzon, B., Mullan, M.A., Keegan, A.P., Parrish, J. *et al.* (2008) Diagnostic utility of APOE, soluble CD40, CD40L, and Abeta1-40 levels in plasma in Alzheimer's disease. *Cytokine*, **44**, 283–287.
73. Obregon, D., Hou, H., Bai, Y., Nikolic, W.V., Mori, T., Luo, D., Zeng, J., Ehrhart, J., Fernandez, F., Morgan, D. *et al.* (2008) CD40L disruption enhances Abeta vaccine-mediated reduction of cerebral amyloidosis while minimizing cerebral amyloid angiopathy and inflammation. *Neurobiol. Dis.*, **29**, 336–353.
74. Laporte, V., Ait-Ghezala, G., Volmar, C.H. and Mullan, M. (2006) CD40 deficiency mitigates Alzheimer's disease pathology in transgenic mouse models. *J. Neuroinflammation*, **3**, 3.
75. Nichol, K.E., Poon, W.W., Parachikova, A.I., Cribbs, D.H., Glabe, C.G. and Cotman, C.W. (2008) Exercise alters the immune profile in Tg2576 Alzheimer mice toward a response coincident with improved cognitive performance and decreased amyloid. *J. Neuroinflammation*, **5**, 13.
76. Hou, H., Obregon, D., Lou, D., Ehrhart, J., Fernandez, F., Silver, A. and Tan, J. (2008) Modulation of neuronal differentiation by CD40 isoforms. *Biochem. Biophys. Res. Commun.*, **369**, 641–647.
77. Zou, J., Yao, Z., Zhang, G., Wang, H., Xu, J., Yew, D.T. and Forster, E.L. (2008) Vaccination of Alzheimer's model mice with adenovirus vector

containing quadrivalent foldable Abeta(1-15) reduces Abeta burden and behavioral impairment without Abeta-specific T cell response. *J. Neurol. Sci.*, **272**, 87–98.
78. Qu, B.X., Xiang, Q., Li, L., Johnston, S.A., Hynan, L.S. and Rosenberg, R.N. (2007) Abeta42 gene vaccine prevents Abeta42 deposition in brain of double transgenic mice. *J. Neurol. Sci.*, **260**, 204–213.
79. Asami-Odaka, A., Obayashi-Adachi, Y., Matsumoto, Y., Takahashi, H., Fukumoto, H., Horiguchi, T., Suzuki, N. and Shoji, M. (2005) Passive immunization of the Abeta42(43) C-terminal-specific antibody BC05 in a mouse model of Alzheimer's disease. *Neurodegener. Dis.*, **2**, 36–43.
80. Li, S.B., Wang, H.Q., Lin, X., Xu, J., Xie, Y., Yuan, Q.F. and Yao, Z.B. (2005) Specific humoral immune responses in rhesus monkeys vaccinated with the Alzheimer's disease-associated beta-amyloid 1-15 peptide vaccine. *Chin. Med. J. (Engl.)*, **118**, 660–664.
81. Lemere, C.A., Beierschmitt, A., Iglesias, M., Spooner, E.T., Bloom, J.K., Leverone, J.F., Zheng, J.B., Seabrook, T.J., Louard, D., Li, D. *et al.* (2004) Alzheimer's disease abeta vaccine reduces central nervous system abeta levels in a non-human primate, the Caribbean vervet. *Am. J. Pathol.*, **165**, 283–297.
82. Hsiao, K., Chapman, P., Nilsen, S., Eckman, C., Harigaya, Y., Younkin, S., Yang, F. and Cole, G. (1996) Correlative memory deficits. A beta elevation, and amyloid plaques in transgenic mice. *Science*, **274**, 99–102.
83. Raivich, G., Gehrmann, J. and Kreutzberg, G.W. (1991) Increase of macrophage colony-stimulating factor and granulocyte–macrophage colony-stimulating factor receptors in the regenerating rat facial nucleus. *J. Neurosci. Res.*, **30**, 682–686.
84. Manczak, M., Park, B.S., Jung, Y. and Reddy, P.H. (2004) Differential expression of oxidative phosphorylation genes in patients with Alzheimer's disease: implications for early mitochondrial dysfunction and oxidative damage. *Neuromolecular Med.*, **5**, 147–162.
85. Gutala, R.V. and Reddy, P.H. (2004) The use of real-time PCR analysis in a gene expression study of Alzheimer's disease post-mortem brains. *J. Neurosci. Methods*, **132**, 101–107.
86. Wilcock, D.M., Gordon, M.N. and Morgan, D. (2006) Quantification of cerebral amyloid angiopathy and parenchymal amyloid plaques with Congo red histochemical stain. *Nat. Protoc.*, **1**, 1591–1155.